44p

437

[redacted]

Copy.
RM L58B25

NACA RM L58B25

Classification changed to declassified
effective 1 April 19[illegible]
authority of NASA C[illegible] 2 by
J. J. Carroll.

[redacted]

N63-13882
Code 1

RESEARCH MEMORANDUM

EFFECT OF CONTROL TRAILING-EDGE THICKNESS OR ASPECT RATIO ON THE OSCILLATING HINGE-MOMENT AND FLUTTER CHARACTERISTICS OF A FLAP-TYPE CONTROL AT TRANSONIC SPEEDS

By William C. Moseley, Jr., and Robert F. Thompson

Langley Aeronautical Laboratory
Langley Field, Va.

OTS PRICE

XEROX $ 4.60 ph

MICROFILM $ 1.52 mf

CLASSIFIED DOCUMENT

This material contains information affecting the National Defense of the United States within the meaning of the espionage laws, Title 18, U.S.C., Secs. 793 and 794, the transmission or revelation of which in any manner to an unauthorized person is prohibited by law.

NATIONAL ADVISORY COMMITTEE FOR AERONAUTICS

WASHINGTON

April 23, 1958

[redacted]

 UNC[redacted]SIFIED

NATIONAL ADVISORY COMMITTEE FOR AERONAUTICS

RESEARCH MEMORANDUM

EFFECT OF CONTROL TRAILING-EDGE THICKNESS OR ASPECT RATIO ON THE OSCILLATING HINGE-MOMENT AND FLUTTER CHARACTERISTICS OF A FLAP-TYPE CONTROL AT TRANSONIC SPEEDS

By William C. Moseley, Jr., and Robert F. Thompson

SUMMARY

Free-oscillation tests were made in the Langley high-speed 7- by 10-foot tunnel to determine the effect of control trailing-edge thickness and control aspect ratio on the dynamic hinge-moment characteristics of a trailing-edge, flap-type control. The semispan-wing—control model had an aspect ratio of 1.80, a taper ratio of 0.74, 0° sweep of the 0.40-chord line, and a modified NACA 64A004 airfoil section. The total control chord was 30 percent of the wing chord, and the controls were hinged at the 0.778 wing-chord line. Tests at Mach numbers from 0.60 to 1.01 were made for a range of oscillation reduced frequency at an angle of attack of 0°.

Aerodynamic damping in the control rotational mode was unstable for the original or basic control configuration previously investigated. Results of the present investigation indicate that either increases in control trailing-edge thickness or decreases in control aspect ratio had a beneficial or stabilizing effect on the control aerodynamic damping. The variation of the aerodynamic damping derivative with oscillation amplitude was generally nonlinear and the amplitude over which the damping was stable increased with increasing trailing-edge thickness or decreasing aspect ratio. The one-degree-of-freedom control-surface flutter of the model could be eliminated for all test conditions by proper choice of control trailing-edge thickness or control aspect ratio. Oscillating the control had only small effects on the aerodynamic in-phase or spring-moment derivatives for the test range of control parameters. The magnitude of the variation in spring-moment derivative with Mach number at transonic speeds was decreased by increasing the control trailing-edge thickness or decreasing the control aspect ratio. The effect of control aspect ratio on the dynamic hinge-moment derivatives is in qualitative agreement with existing unsteady flow theory.

[redacted]

INTRODUCTION

Oscillatory hinge-moment data on flap-type controls are needed in flutter and servo-control analyses. These data are of particular interest at transonic speeds where previous work has shown that the aerodynamic damping in the control rotational mode is often unstable. A single-degree-of-freedom control-surface flutter (often called "buzz") can exist if this unstable aerodynamic damping exceeds the stable damping from nonaerodynamic sources. The addition of sufficient nonaerodynamic damping to the control system to prevent flutter generally results in mechanical complexities and it would therefore be desirable to stabilize the control aerodynamic moments by some choice in geometric shape if control efficiency can be maintained.

The investigations reported in references 1 to 3 were made on an unswept wing-control model to study the effects of control hinge-line position and some control-profile modifications on the control oscillating hinge moments. From these investigations, it was determined that some beneficial effect on the control aerodynamic damping at transonic speeds was obtained with a control profile, wherein the control was thicker at the trailing edge than at the hinge line.

The present investigation is essentially a continuation of the work reported in references 1 to 3. The same wing-control model was used and two groups of tests were made. One part of the investigation was to study control-profile effects, wherein the controls tested had trailing edges thicker than the control previously reported in reference 3. A second part of the investigation provided information on control-aspect-ratio effects, wherein conventional-profile controls were tested and the control span was reduced relative to that of the controls previously investigated by cutting off the outboard portion of the control. The effects of control aspect ratio were considered of interest, since theoretical results reported in references 4, 5, and 6 indicate that reducing the aspect ratio has a stabilizing effect on the damping due to harmonic oscillations in pitch of rectangular surfaces (wings and ailerons) at high transonic and supersonic speeds. It should be pointed out, however, that the aspect-ratio modification to the present control introduces control spanwise position as a test variable in addition to the changes in control aspect ratio.

A free-oscillation-test technique was used and oscillating hinge moments were determined at an angle of attack of 0° for the following conditions: a range of control reduced frequencies, oscillation amplitudes up to 13°, and a Mach number range from 0.60 to 1.01. For cases where control flutter occurred, flutter amplitudes and frequency were determined. In addition, static hinge moments were obtained for all controls.

SYMBOLS

A control aspect ratio (control span squared divided by total control area)

b twice span of semispan model, ft

c local wing chord, ft

c_a local control chord (distance from hinge line rearward to trailing edge of control), ft

c_b local balance chord (distance from hinge line forward to leading edge of control), ft

c_t total local control chord, $(c_b + c_a)$, ft

C_h control hinge-moment coefficient, $\frac{\text{Hinge moment}}{2M'q}$

$C_{h_\delta} = \frac{\partial C_h}{\partial \delta}$

$$\left.\begin{aligned} C_{h_{\delta,\omega}} &= \frac{\text{Real part of } M_\delta}{2M'q}, \text{ per radian} \\ C_{h_{\dot{\delta},\omega}} &= \frac{\text{Imaginary part of } M_\delta}{2M'qk}, \text{ per radian} \end{aligned}\right\} \text{ the subscript } \omega \text{ indicates an oscillatory coefficient}$$

f frequency of control oscillation, cps

f_o control wind-off natural frequency, cps

I moment of inertia of control system, slug-ft^2

k control reduced frequency $\frac{\omega c_t}{2V}$, where c_t is taken at mid-span of control

M effective test Mach number over span of model, $\frac{2}{S_1}\int_0^{b/2} cM_a \, dy$

M_a average chordwise local Mach number

[redacted]

M'	area moment of control area rearward of and about hinge line, cu ft
M_δ	aerodynamic hinge moment on control per unit deflection, positive trailing edge down, ft-lb/radian
q	free-stream dynamic pressure, lb/sq ft
S_1	twice wing area of semispan model, sq ft
V	free-stream velocity, ft/sec
y	spanwise distance from plane of symmetry, ft
δ	control-surface deflection, measured in a plane perpendicular to control-surface hinge line, positive when control-surface trailing edge is below wing-chord plane, radians except as noted otherwise
δ_1	amplitude of control oscillation, degrees to each side of mean control deflection
λ	logarithmic decrement, $\frac{d(\log \delta_1)}{d(\text{time})}$, per second
ϕ	control trailing-edge angle (included between sides which form trailing edge), deg
ω	angular frequency of oscillation, $2\pi f$, radians/sec

MODEL AND APPARATUS

The model consisted of a semispan wing with tip store, a trailing-edge flap-type control, and a control-system spring-deflector mechanism. A schematic drawing of the test installation is shown in figure 1, and general dimensions of the model with various controls tested are given in figure 2. A photograph showing the general test installation in the tunnel is shown as figure 3. The control system was designed so that its moment of inertia could be varied in order to measure the dynamic hinge moments and flutter characteristics for a range of control reduced frequency.

Wing Details

The wing had a full-span aspect ratio of 1.80, a taper ratio of 0.74, 0° sweep of the 0.40 chord line, and an NACA 64A004 airfoil section with a modified trailing edge. The portion of the wing rearward of the 0.70 chord line was modified so that the trailing edge had a thickness equal to 0.0036c. This modification was included for the present tests to provide consistency with the models tested in references 1 to 3.

The wing was constructed with a solid steel core and a plastic surface. All tests were made with a tip store attached to the wing, and stores of different weight were used to vary the wing natural frequencies. The natural first bending and torsion frequencies of the wing with the two tip stores are given in table I. These frequencies were obtained with the control system spring clamped as shown in figure 1.

Control-System Details

The flap-type controls had a total chord c_t equal to 30 percent of the wing chord and were hinged at the 0.778 wing-chord line. The controls had a $0.35c_a$ blunt-overhang balance and the gap between the control and the wing was unsealed. The thickened trailing-edge controls (fig. 2(a)) extended from the 0.086b/2 wing station to the 0.943b/2 wing station. These controls, which are referred to as "wedge controls," had straight sides from the nose radius to the trailing edge. The included angle ϕ between the upper and lower surface was 6.5° for one wedge and 10° for the other. The controls had a steel spar and a spruce afterportion. In order to mass balance the controls, tungsten inserts were distributed in the nose overhang and the entire control surface was wrapped with silk.

The reduced-aspect-ratio controls (fig. 2(b)) extended from the 0.086b/2 wing station to either the 0.692b/2 wing station or the 0.433b/2 wing station. These controls were made of steel and the control profile was mainly determined by the model airfoil section. In addition to the tungsten inserts it was necessary to drill holes rearward of the hinge line in order to mass balance the steel controls completely. These holes were filled with balsa before the control was covered with silk.

A tang on the inboard end of the control extended through the reflection plane to the outside of the tunnel (fig. 1). The tang extension consisted of a rod and a torsion spring. The control was mounted by two ball bearings outside the tunnel and a plain bearing at the wing tip. System alinement was carefully checked to keep friction to a minimum. Attached to the rod were a small armature of a reluctance-type pickup used to indicate control position and a deflector arm used to

apply a step deflection to the control system. The natural frequency of the control system was varied by changing the moment of inertia of the control system by clamping weights of different size and inertia to the rod. The moments of inertia of the control system for the controls tested are given in table II. The variation of control-system stiffness and the wind-off natural frequencies are given in figure 4 for the various controls.

Instrumentation

Strain gages were located near the root of the wing to indicate the wing bending and torsion responses. Control position was measured by the reluctance-type pickup located near the inboard end of the control. (See sketch in fig. 4.) Outputs of these three quantities were recorded against time by a recording oscillograph. Dynamic calibration of the recording system indicated accurate response to a frequency of about 500 cycles per second.

TESTS

The tests were made in the Langley high-speed 7- by 10-foot tunnel utilizing the sidewall reflection-plane test technique. This technique involves mounting a relatively small model on a reflection plate spaced out from the tunnel wall to bypass the tunnel boundary layer. Local velocities over the surface of the test reflection plate allowed testing to a Mach number of 1.01 without choking the tunnel. The tunnel stagnation pressure was essentially equal to sea-level atmospheric pressure.

The variation of Reynolds number based on the wing mean aerodynamic chord with test Mach number is presented in figure 5. The width of the band in figure 5 represents the maximum variation of Reynolds number with atmospheric condition at a given Mach number.

Oscillating hinge moments were obtained for the controls through a Mach number range of 0.60 to 1.01 for oscillation amplitudes up to about 13°. The range of control reduced frequency k varied with Mach number and control-system inertia and was generally in the range from 0.05 to 0.20. In addition, static hinge moments were obtained for all controls. All tests were made at a wing angle of attack of 0°.

TEST TECHNIQUE AND REDUCTION OF DATA

The control system was designed so that at the test frequencies the torsional response of the control about the hinge line was essentially

that of a single-degree-of-freedom system. The wing response characteristics were varied relative to the control oscillation frequency by the choice of tip-store weight so that the physical response of the model for the various test conditions was predominantly control rotation. Therefore, the aerodynamic moment resulting from angular deflection of the control about the hinge line could be determined from the free-oscillation characteristics of the control system subsequent to known starting conditions. Typical oscillograph records of the time response of the model are shown in figure 6. In this figure, the wing motions indicated are small relative to the control motions. The mean oscillation amplitude for this investigation was very near 0° deflection in all cases.

The technique used to initiate the free oscillations depended on the total damping (aerodynamic plus nonaerodynamic) of the control system for the particular test condition. When the total damping was unstable at low deflections, the hinge moments were determined from the unstable oscillation following release of the control at $\delta \approx 0^{\circ}$ (fig. 6(c)). This type of oscillation was initiated by random tunnel disturbances and in all cases tested was self-limiting. When the total damping was stable or varied from stable to unstable within the test oscillation-amplitude range, the free oscillation was initiated by releasing the control at some deflection angle (figs. 6(a) and (b)). The ensuing oscillation was either a buildup or a decay, and, for the conditions where the damping varied from stable to unstable, the initial deflection or release angle was varied so as to study the entire oscillation-amplitude range.

Evaluation of Spring Moments

The aerodynamic in-phase or spring moment was determined from the natural frequency of oscillation of the control system. Since the variation of in-phase moment with amplitude is not necessarily linear and the test method was not sufficiently accurate to determine the variation in natural frequency with amplitude, the values of $C_{h_{\delta,\omega}}$ presented are effective values averaged over the amplitude range of the oscillation. In this investigation, the effect of the values of damping on the natural frequency was considered negligible, and the aerodynamic spring-moment derivative was determined from the relationship

$$C_{h_{\delta,\omega}} = \frac{I\left(\omega_o^2 - \omega^2\right)}{2M'q} \tag{1}$$

where the subscript o signifies a wind-off condition. As shown by equation (1), negative values of $C_{h_{\delta,\omega}}$ oppose the control displacement and hence increase the stiffness or natural frequency of the control surface.

Evaluation of Damping Moments

The aerodynamic out-of-phase or damping moment was determined from the rate of buildup or decay of the free oscillation of the control system. The damping moment is not necessarily linear with amplitude; however, the damping results were analyzed on the basis of an equivalent linear system. It was assumed that the damping forces were adequately described by an equivalent viscous damping and that the time response of the actual system was simulated by a linear system having the appropriate damping constant at each oscillation amplitude for a given frequency. The variation of damping-moment derivative with oscillation amplitude was obtained by plotting the logarithm of the amplitude of successive cycles of the oscillation against time and taking the slope at any given amplitude of the faired curves as the value of the logarithmic decrement $\lambda = \frac{d(\log \delta_1)}{d(\text{time})}$ of the oscillation. The aerodynamic damping derivative was determined from the relationship

$$C_{h_{\dot{\delta},\omega}} = \frac{2IV}{qM'c_t}\left(\lambda - \lambda_o\right) \tag{2}$$

where the subscript o refers to wind-off values taken at approximately the same frequency and amplitude as the wind-on values.

Determination of Static Hinge Moments

Static hinge moments were measured by restraining the control system in torsion with a calibrated electric strain gage which measured the torque or moment about the control hinge line for various control deflections. The static hinge-moment coefficient C_h was determined from the relationship

$$C_h = \frac{\text{Hinge moment}}{2M'q} \tag{3}$$

CORRECTIONS

No corrections have been applied to the data for the chordwise and spanwise velocity gradients or for the effects of the tunnel walls. It is shown in reference 7 that a tunnel resonance phenomenon can appreciably decrease the magnitude of forces and moments measured in oscillation tests. However, it is believed that this phenomenon had no appreciable effect on the results of the present investigation. In general, most of the test

frequencies were well removed from the calculated resonant frequencies, and there was no apparent decrease in moments for the test frequencies that were close to resonant frequencies. It is possible that the magnitude of the resonant effects would be relieved by the model tip effects and the nonuniformity of the velocity field in the test section.

Static-control-deflection corrections have been applied to the output of the position pickup to give the deflection at the midspan of the control surface for the static tests. No dynamic corrections have been applied to the oscillatory data to account for the twist of the control system outboard of the position pickup (fig. 4) since, for the physical constants and frequencies involved, this was considered a secondary effect.

RESULTS AND DISCUSSION

Damping Moments and Flutter Characteristics

The variation of aerodynamic damping derivative $C_{h_{\dot{\delta},\omega}}$ with oscillation amplitude and Mach number together with associated flutter characteristics is presented in figures 7 and 8 for the wedge controls and in figures 9 and 10 for the reduced-aspect-ratio controls. Parts (a), (b), and (c) of these figures present data for the different control reduced frequencies investigated. In figures 11 and 12 typical aerodynamic damping results from the present investigation are compared with previously reported results from reference 3 to illustrate the effects of the changes in control geometry investigated.

Wedge controls.- As shown in figure 11, the aerodynamic damping in the control rotational mode was unstable for the conventional control profile. Results of the present investigation indicate that increases in the control trailing-edge thickness had a beneficial or stabilizing effect on this control aerodynamic damping. The general variation of damping derivative with oscillation amplitude and Mach number for the $\phi = 6.5^{\circ}$ and 10° wedge controls reported herein (figs. 7 and 8) was similar to the variation previously reported in reference 3 for a $\phi = 3.75^{\circ}$ wedge control, and the primary effect of increasing the control wedge angle above 3.75° was to increase the oscillation amplitude over which the control aerodynamic damping was stable at transonic test speeds.

Aerodynamic damping for the $\phi = 6.5^{\circ}$ wedge control (fig. 7) was stable at all test conditions for oscillation amplitudes up to about 6°, and there was a general tendency for the level of stable damping to decrease with an increase in either test Mach number or oscillation amplitude. The variation of $C_{h_{\dot{\delta},\omega}}$ with amplitude was usually more

nonlinear at transonic Mach numbers and the variation of $C_{h_{\dot{\delta},\omega}}$ with Mach number was erratic at these speeds. Decreasing the test reduced frequency generally had a destabilizing effect on the aerodynamic damping, especially at higher oscillation amplitudes at transonic Mach numbers.

Aerodynamic damping for the $\phi = 10^{\circ}$ wedge control (fig. 8) was stable for all test conditions. At the high reduced frequency (fig. 8(a)) there was no tendency for the damping derivative to decrease with increasing oscillation amplitude at transonic speeds; however, $C_{h_{\dot{\delta},\omega}}$ did decrease with increasing amplitude at the lower reduced frequencies (figs. 8(b) and 8(c)) with the aerodynamic damping near neutral for the higher test amplitudes at transonic speeds.

No model flutter was obtained for either of the wedge controls reported herein. For the large-control-deflection conditions where the aerodynamic damping was slightly unstable for the $\phi = 6.5^{\circ}$ wedge control, the stable damping from nonaerodynamic sources present in the control system was sufficient to prevent flutter.

Reduced aspect-ratio controls.- The controls used for the aspect-ratio-effects investigation had so-called conventional profiles dictated by the wing airfoil section. Data for the aspect-ratio-2.55 control (fig. 12) were obtained from reference 3, wherein the control covered a large portion of the test model span. The 1.74- and 0.96-aspect-ratio controls of the present investigation (figs. 9, 10, and 12) were essentially modifications to the control of reference 3 with the position of the inboard end of the control common for all three controls.

Aerodynamic damping for the aspect-ratio-1.74 control (fig. 9) was stable for all test oscillation amplitudes for Mach numbers up to 0.94. Increasing the test Mach number above about 0.90 had a large destabilizing effect on the aerodynamic damping for this control and the damping was unstable in the test speed range from about $M = 0.95$ to $M = 1.01$, the maximum speed for this investigation. Decreasing the test reduced frequency generally increased the magnitude of the unstable aerodynamic damping derivative $C_{h_{\dot{\delta},\omega}}$. In the test region where the aerodynamic damping was unstable, $C_{h_{\dot{\delta},\omega}}$ decreased with increasing amplitude and a limited amplitude, single-degree-of-freedom model flutter response occurred. Flutter was initiated in all cases by random tunnel disturbances upon release of the control system and the flutter amplitude as indicated in the model flutter tables on figure 9 varied with Mach number, reduced frequency, and the level of nonaerodynamic damping existing in the control system.

Aerodynamic damping for the aspect-ratio-0.96 control (fig. 10) was stable for all test conditions except for the small region shown on

figure 10(c). In this case, for the lowest reduced frequencies of the tests, small unstable values of $C_{h_{\dot{\delta},\omega}}$ were obtained at the higher test Mach numbers for oscillation amplitudes less than about 2°. The model did not flutter for these test conditions since the stable nonaerodynamic damping present in the system was sufficient to overcome the small amount of unstable aerodynamic damping.

The summary results shown in figure 12 for representative test conditions illustrate the stabilizing effect on the aerodynamic damping in the control rotational mode at transonic speeds due to decreasing the control aspect ratio on this model. Similar stabilizing effects due to decreasing aspect ratio have been obtained for results computed by linearized theory for compressible unsteady flow. These calculated results for the aerodynamic damping due to harmonic oscillations in pitch of rectangular surfaces may be found in references 4, 5, and 6. References 4 and 5 treat the finite rectangular wing and reference 6 is essentially an extension of reference 5 to include a rectangular aileron. It is considered of interest to compare the results computed for supersonic flow in references 5 and 6 with the high Mach number test results of the present investigation, since model thickness increases the local surface velocities over the model. Results of reference 1 for the test model indicate that local surface velocities exceed $M = 1.0$ for free-stream velocities in excess of $M = 0.90$. In computing the loading on a finite surface in supersonic flow, the surface is divided into regions of "purely supersonic" and "mixed supersonic" flow. (See, for example, ref. 8.) For the case of the present experimental investigation where the wing remains essentially stationary at $\alpha = 0^{\circ}$, the "mixed supersonic" flow region on the control surface lies within the Mach cone emanating from the control tip. Of particular significance to the present investigation are the theoretical results at low supersonic speeds, which indicate a stable phase angle for the damping moment associated with the loading in the "mixed supersonic" flow region and an unstable phase angle for the moment in the "purely supersonic" flow region. Since for a given supersonic Mach number, decreasing the control aspect ratio increases the ratio of "mixed supersonic" to "purely supersonic" flow over the control surface, the stabilizing effect due to aspect ratio becomes apparent. At these higher test speeds, the effects of control spanwise position are believed to be small relative to the aspect-ratio effects for the test conditions of this model. Control tip boundary conditions were similar for all control spans and the influence of the upstream wing on the control oscillatory loads would probably be small at these speeds.

As is usually the case, several differences exist between experimental and theoretical conditions. Contrary to experiment, theory is based on small perturbations to the main flow and the flow is assumed to be nonviscous, unseparated, and free from strong shocks. In addition, the "mixed supersonic" flow region defines the zone of influence between

the upper and lower surfaces. Thus, the loading in this region is influenced by the boundary conditions at the control tip; that is, the loading depends on whether the tip is free or adjacent to a portion of the wing or fuselage. Some compromise is made in the theory (see ref. 8) for the tip-boundary condition where the control is adjacent to the wing as was the case for this experimental investigation. The overall effects of these differences between test and theory are not known. A number of previous investigations (for example, see ref. 9) have associated the unstable damping in the control rotational mode at transonic speeds with the presence of shock waves. The nonlinear nature of the aerodynamic results measured in the present experimental investigation indicate that such possible nonpotential factors as viscosity, separation, and shock waves can have a strong influence on the measured results. However, the qualitative agreement between the general effects of aspect ratio as measured in the present test results and as predicted by existing theory is considered to be significant. A similar conclusion was reached on the effect of hinge-line position in reference 2. Therefore, the present results again tend to indicate that the aerodynamic damping in the control rotational mode is strongly dependent on potential or idealized flow effects and that existing theory can serve as a useful guide.

Spring Moments

Static hinge-moment or spring-moment coefficients are plotted against control deflection in figure 13 for the wedge controls and in figure 14 for the variable-aspect-ratio controls. The variations of the static and dynamic spring-moment derivatives C_{h_δ} and $C_{h_{\delta,\omega}}$ with Mach number are shown in figure 15 for the wedge controls and in figure 16 for the variable-aspect-ratio controls, together with comparative results from reference 3.

Wedge controls.- The variation of C_h with δ was similar for both the $\phi = 6.5^\circ$ and $\phi = 10^\circ$ wedge controls (fig. 13) and was fairly linear for a deflection range of about $\pm 5^\circ$ throughout the Mach number range. Static derivatives (fig. 15) for the wedge controls were averaged over this approximate deflection range, and the effects of wedge angle for the range of the tests to date on this model can be determined by comparing results in figure 15 with the aspect-ratio-2.55, conventional-profile-control results shown on figure 16. The wedge modification to the profile shifts C_{h_δ} in a negative direction (more underbalanced) in the subsonic speed range with most of the shift occurring for the $\phi = 3.75^\circ$ control. At transonic speeds, wedge angle has generally small effects but in the opposite direction (increasing ϕ shifts C_{h_δ} in a positive direction). Thus the magnitude of the typical rearward chordwise shift in control loading as the Mach number is increased from subsonic to supersonic flow is reduced by increasing the control

divergence wedge angle. As a result of the type of test technique used, it was generally necessary to average the oscillating spring-moment derivatives over a different deflection range than the static derivatives. This could introduce some differences in the static and dynamic spring-moment derivatives as presented. However, for the range of these tests, oscillating the control generally had small effects on the aerodynamic spring-moment derivatives. Thus, fairly accurate control frequency response estimates could be made for these wedge controls based on static aerodynamic spring-moment derivatives.

Variable aspect-ratio controls.- Static derivatives for the reduced aspect-ratio controls (fig. 16) were also averaged over a deflection range of about $\pm 5^{\circ}$ (fig. 14). Decreasing the control aspect ratio generally had a balancing (positive increase in the derivative) effect on both the static and oscillating spring-moment derivatives, with the effect becoming quite large at the higher test Mach numbers. At subsonic test speeds, some of this effect could possibly be due to control spanwise position, since the loading induced on the wing and control would be affected by the flow about the wing tip. However, at the higher test speeds where the local surface velocities become supersonic, the effect of control spanwise position is believed to be small from consideration of the fact that the control-tip boundaries are similar for all three controls. This balancing tendency with decreased aspect ratio is probably associated with the decrease in loading due to flow about the control tips, the relative magnitude of which increases as the control aspect ratio decreases. For the combination of hinge-line position and aspect ratios of the test controls, decreasing the control aspect ratio to 0.96 (fig. 16) overbalanced the control through a portion of the speed range and for the Mach number range of the tests considerably decreased the rearward chordwise shift in loading generally associated with the transition from subsonic to supersonic speeds. Oscillating these variable aspect-ratio controls generally had small effect on the aerodynamic spring-moment derivatives, and the effect of aspect ratio on the dynamic in-phase derivatives is in qualitative agreement with theoretical results presented in references 4, 5, and 6.

CONCLUSIONS

Results of tests at Mach numbers from 0.60 to 1.01 to determine the effects of either trailing-edge thickness or aspect ratio of controls on the oscillating hinge-moment and flutter characteristics of a flap-type control indicate the following conclusions:

1. Increasing the control trailing-edge thickness had a stabilizing effect on the unstable aerodynamic damping present in the control rotational mode at transonic speeds for the basic control profile. The

variation of aerodynamic damping with oscillation amplitude was nonlinear, and the amplitude over which the damping was stable increased with increasing thickness.

2. Decreasing the control aspect ratio (by cutting off the outboard portion of the control) also had a stabilizing effect on the control aerodynamic damping at transonic speeds. Changing the control aspect ratio from 2.55 to 0.96 generally stabilized the damping for the present test conditions.

3. One-degree-of-freedom control-surface flutter of this model could be eliminated for all test conditions by proper choice of control trailing-edge thickness or control aspect ratio.

4. Oscillating the control had fairly small effects on the aerodynamic in-phase or spring-moment derivatives for the range of control parameters tested.

5. The magnitude of the variation in spring-moment derivative with Mach number at transonic speeds was decreased by increasing the control trailing-edge thickness or decreasing the control aspect ratio.

6. The effect of aspect ratio on the control dynamic hinge-moment derivatives is in qualitative agreement with existing unsteady flow theory.

Langley Aeronautical Laboratory,
National Advisory Committee for Aeronautics,
Langley Field, Va., February 12, 1958.

REFERENCES

1. Thompson, Robert F., and Moseley, William C., Jr.: Oscillating Hinge Moments and Flutter Characteristics of a Flap-Type Control Surface on a 4-Percent-Thick Unswept Wing With Low Aspect Ratio at Transonic Speeds. NACA RM L55K17, 1956.

2. Thompson, Robert F., and Moseley, William C., Jr.: Effect of Hinge-Line Position on the Oscillating Hinge Moments and Flutter Characteristics of a Flap-Type Control at Transonic Speeds. NACA RM L57C11, 1957.

3. Moseley, William C., Jr., and Price, George W., Jr.: Effects of Control Profile on the Oscillating Hinge-Moment and Flutter Characteristics of a Flap-Type Control at Transonic Speeds. NACA RM L57E27, 1957.

4. Runyan, Harry L., and Woolston, Donald S.: Method for Calculating the Aerodynamic Loading on an Oscillating Finite Wing in Subsonic and Sonic Flow. NACA Rep. 1322, 1958. (Supersedes NACA TN 3694.)

5. Nelson, Herbert C., Rainey, Ruby A., and Watkins, Charles E.: Lift and Moment Coefficients Expanded to the Seventh Power of Frequency for Oscillating Rectangular Wings in Supersonic Flow and Applied to a Specific Flutter Problem. NACA TN 3076, 1954.

6. Berman, Julian H.: Lift and Moment Coefficients for an Oscillating Rectangular Wing-Aileron Configuration in Supersonic Flow. NACA TN 3644, 1956.

7. Runyan, Harry L., and Watkins, Charles E.: Considerations on the Effect of Wind-Tunnel Walls on Oscillating Air Forces for Two-Dimensional Subsonic Compressible Flow. NACA Rep. 1150, 1953. (Supersedes NACA TN 2552.)

8. Garrick, I. E., and Rubinow, S. I.: Theoretical Study of Air Forces on an Oscillating or Steady Thin Wing in a Supersonic Main Stream. NACA Rep. 872, 1947. (Supersedes NACA TN 1383.)

9. Henning, Allen B.: Results of a Rocket-Model Investigation of Control-Surface Buzz and Flutter on a 4-Percent-Thick Unswept Wing and on 6-, 9-, and 12-Percent-Thick Swept Wings at Transonic Speeds. NACA RM L53I29, 1953.

TABLE I.- NATURAL FIRST BENDING AND TORSION

FREQUENCIES OF WING

Test Condition		Bending, cps	Torsion, cps
6.5° wedge control	plus light tip store	145	490
	plus heavy tip store	86	228
10° wedge control	plus light tip store	145	490
	plus heavy tip store	86	228
A = 1.74 control	plus light tip store	147	325
	plus heavy tip store	87	232
A = 0.96 control	plus light tip store	148	329
	plus heavy tip store	90	226

TABLE II.- MOMENTS OF INERTIA OF CONTROL SYSTEMS

Control System	I, slug-ft^2
ϕ = 6.5° wedge control	1.50×10^{-5}
ϕ = 6.5° wedge control plus small inertia weight	3.46
ϕ = 6.5° wedge control plus large inertia weight	10.77
ϕ = 10° wedge control	1.33
ϕ = 10° wedge control plus small inertia weight	3.29
ϕ = 10° wedge control plus large inertia weight	10.60
A = 1.74 control	1.42
A = 1.74 control plus small inertia weight	3.39
A = 1.74 control plus large inertia weight	10.70
A = 0.96 control	1.13
A = 0.96 control plus small inertia weight	3.10
A = 0.96 control plus large inertia weight	10.40

UNCLASSIFIED
[redacted]

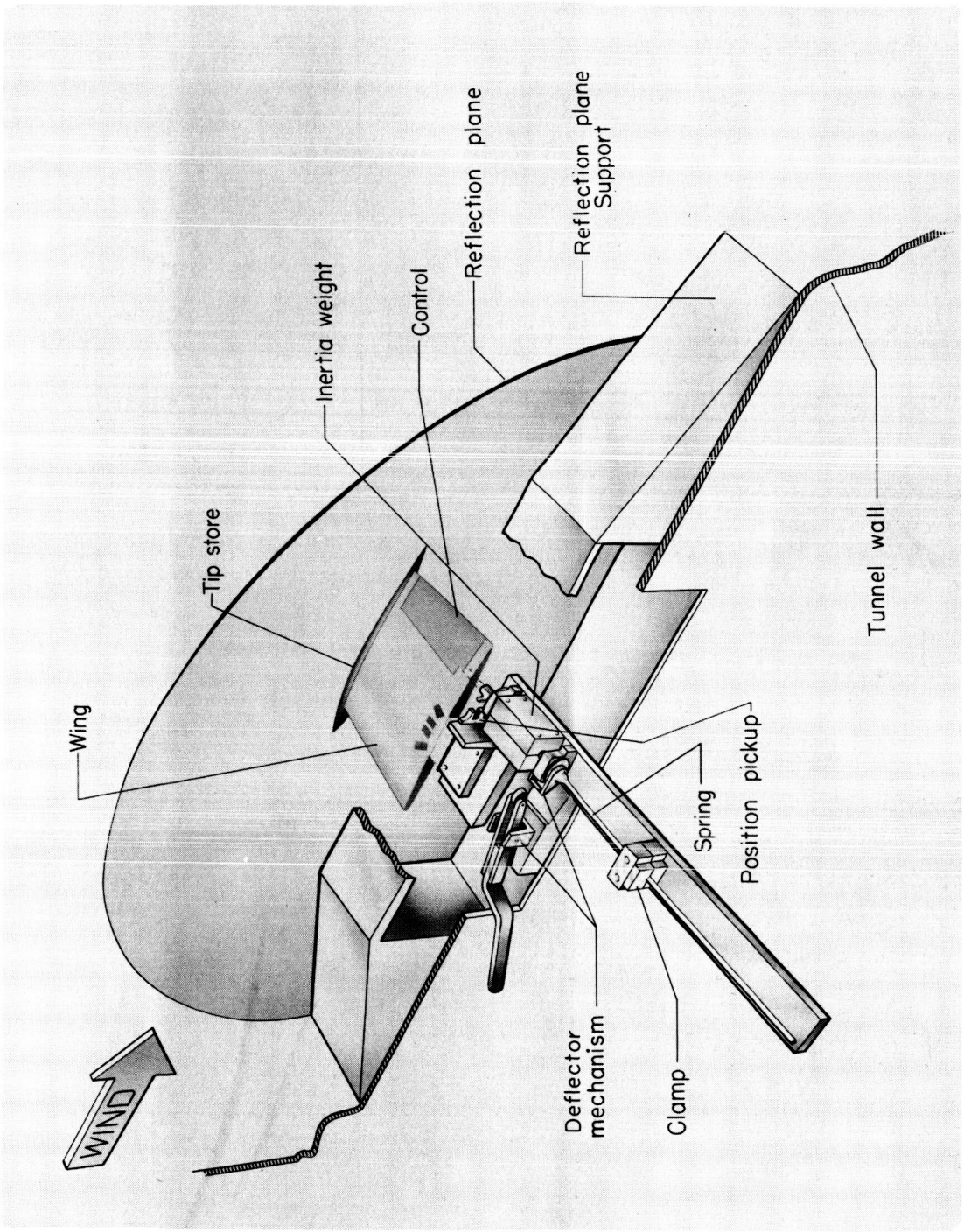

Figure 1.- Schematic drawing of test installation. L-90563.2

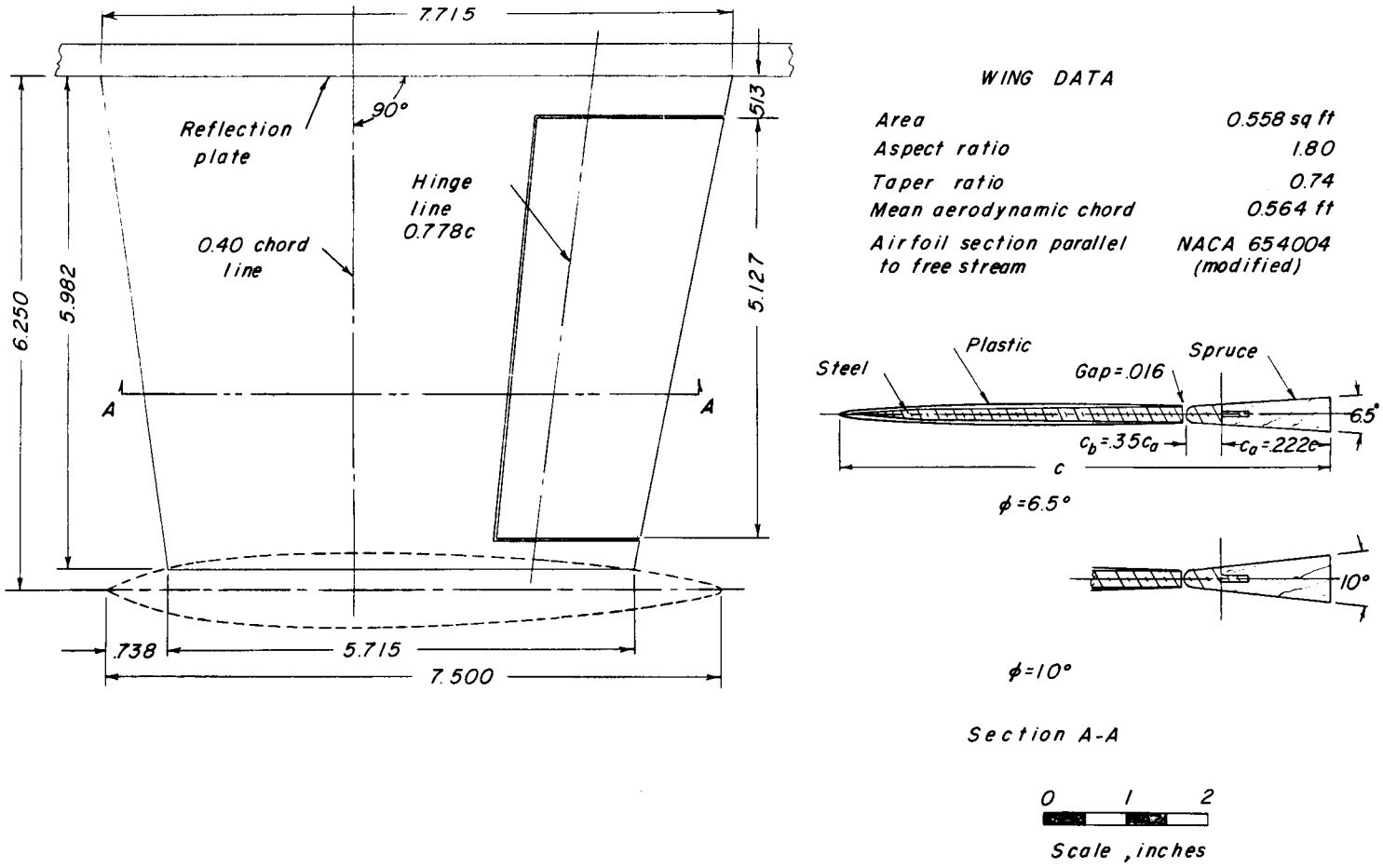

(a) Thickened trailing-edge controls.

Figure 2.- General dimensions of model.

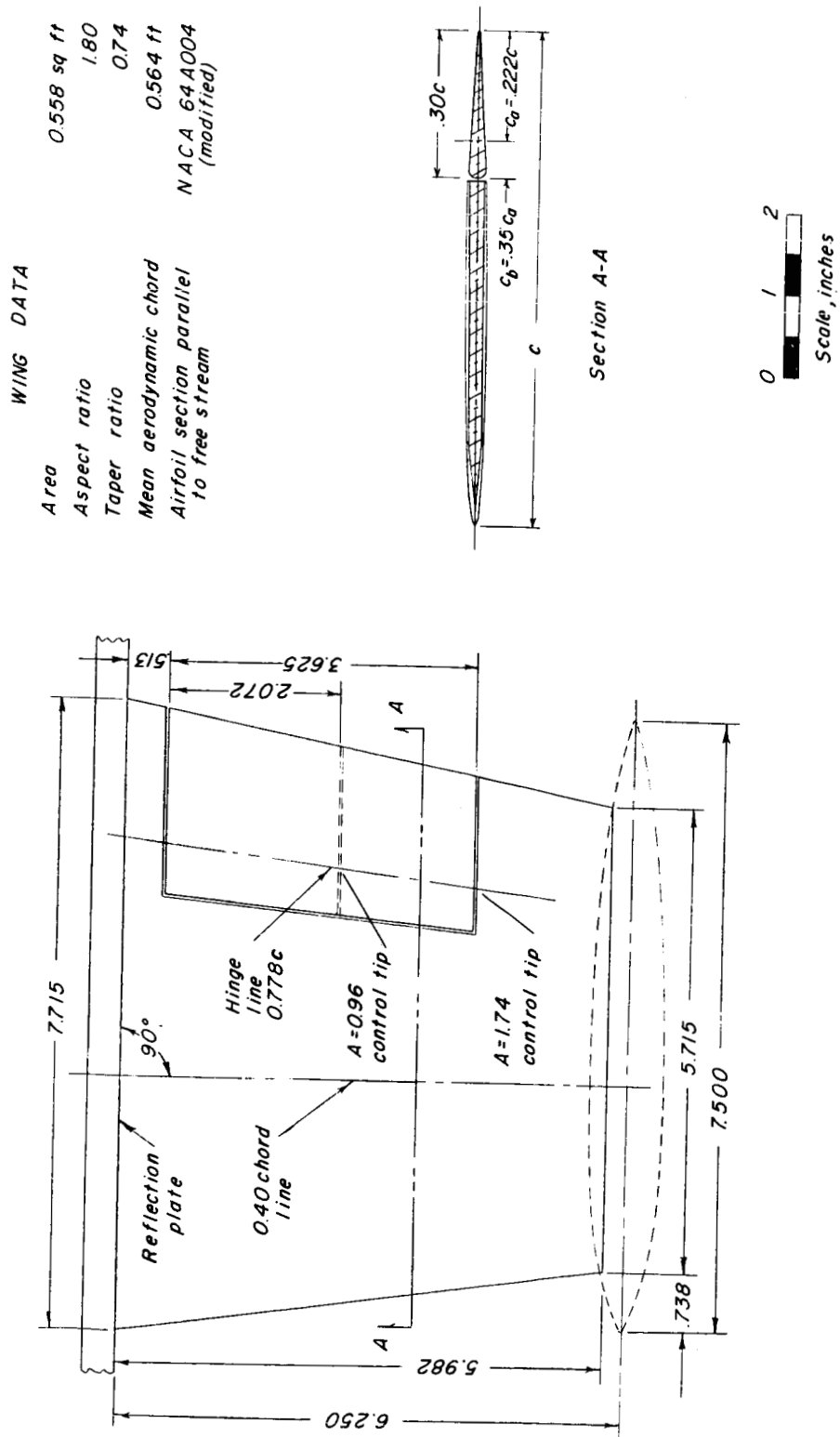

(b) Reduced-aspect-ratio controls.

Figure 2.- Concluded.

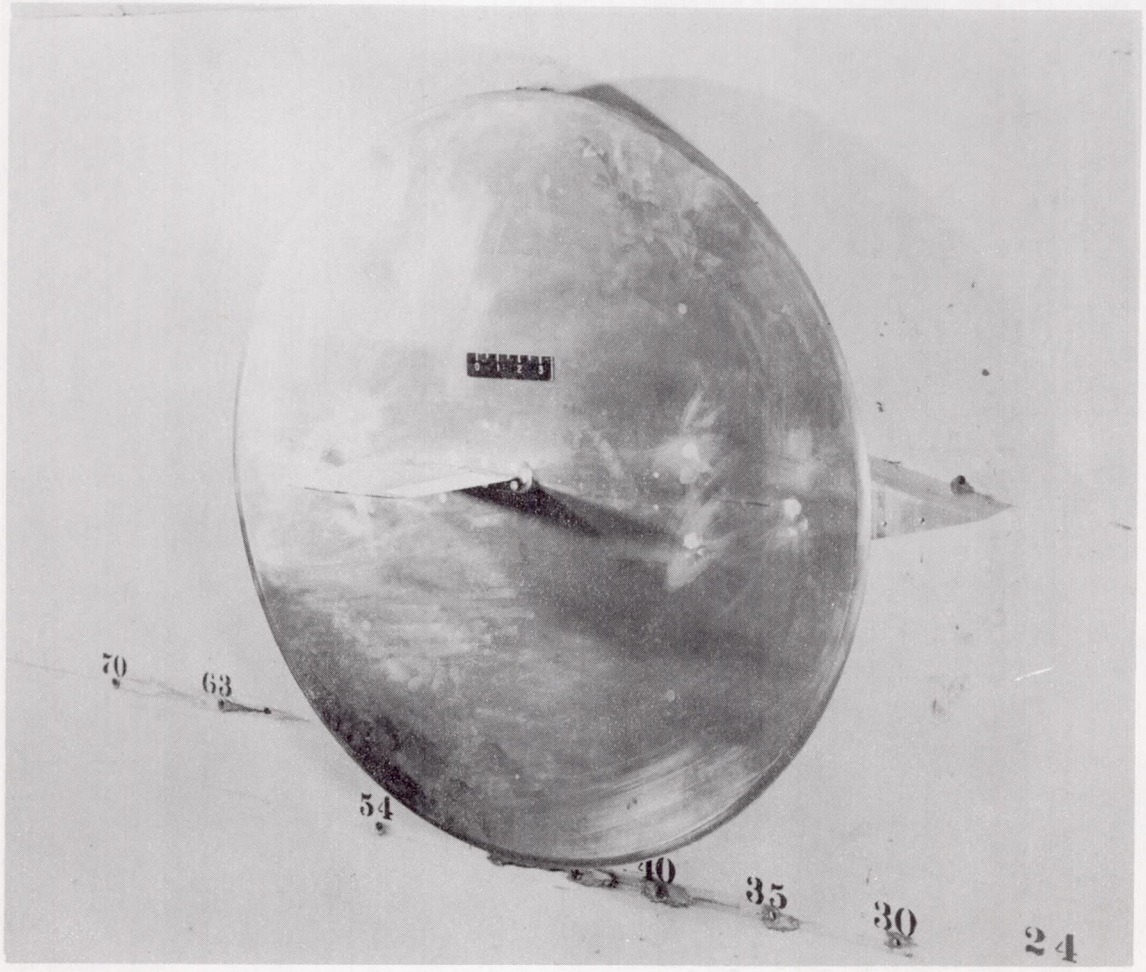

L-86715

Figure 3.- Photograph showing general arrangement of model and reflection plate.

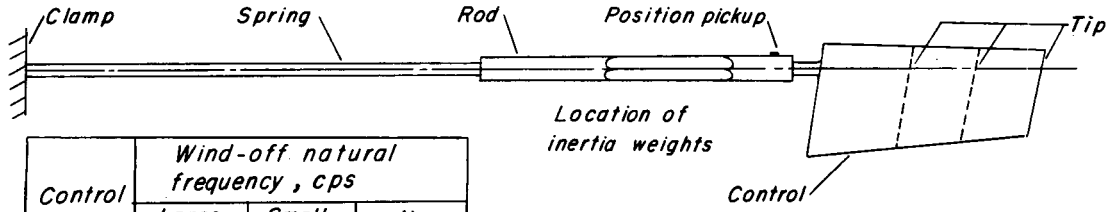

Control	Wind-off natural frequency, cps		
	Large I-weight	Small I-weight	No weight
6.5° wedge	99.0	171.5	253.0
10° wedge	99.0	172.5	250.0
A = 1.74	99.5	174.0	260.0
A = 0.96	102.0	188.0	308.0

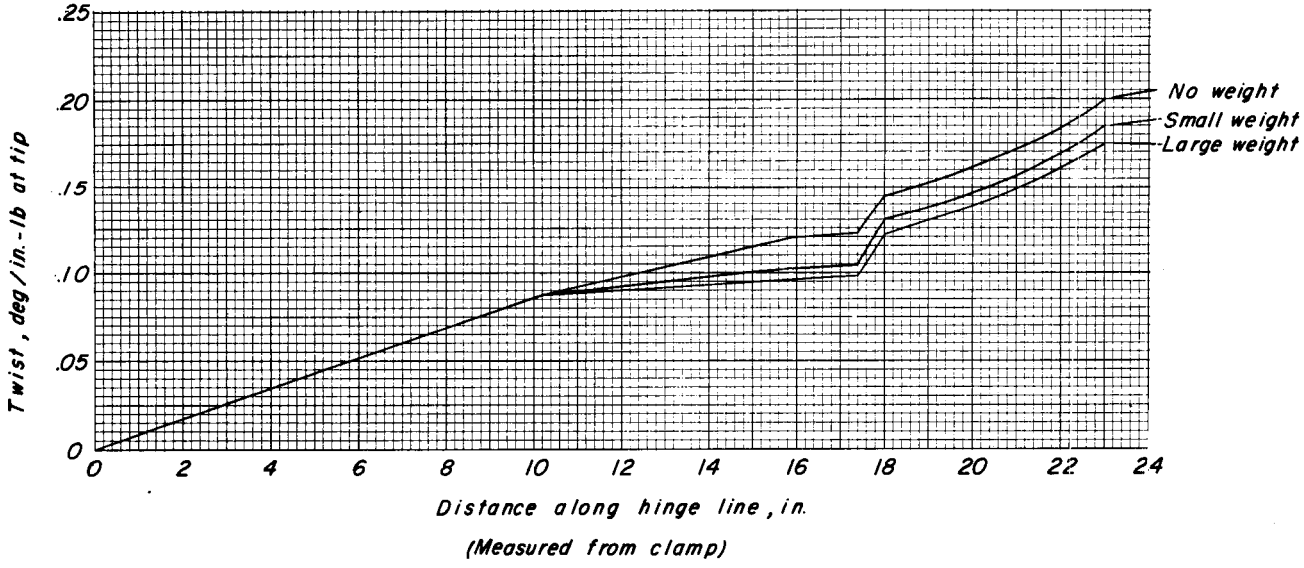

Figure 4.- Control-system stiffness and frequency for various controls and inertia weights. (Stiffness applies to both conventional and wedge profiles.)

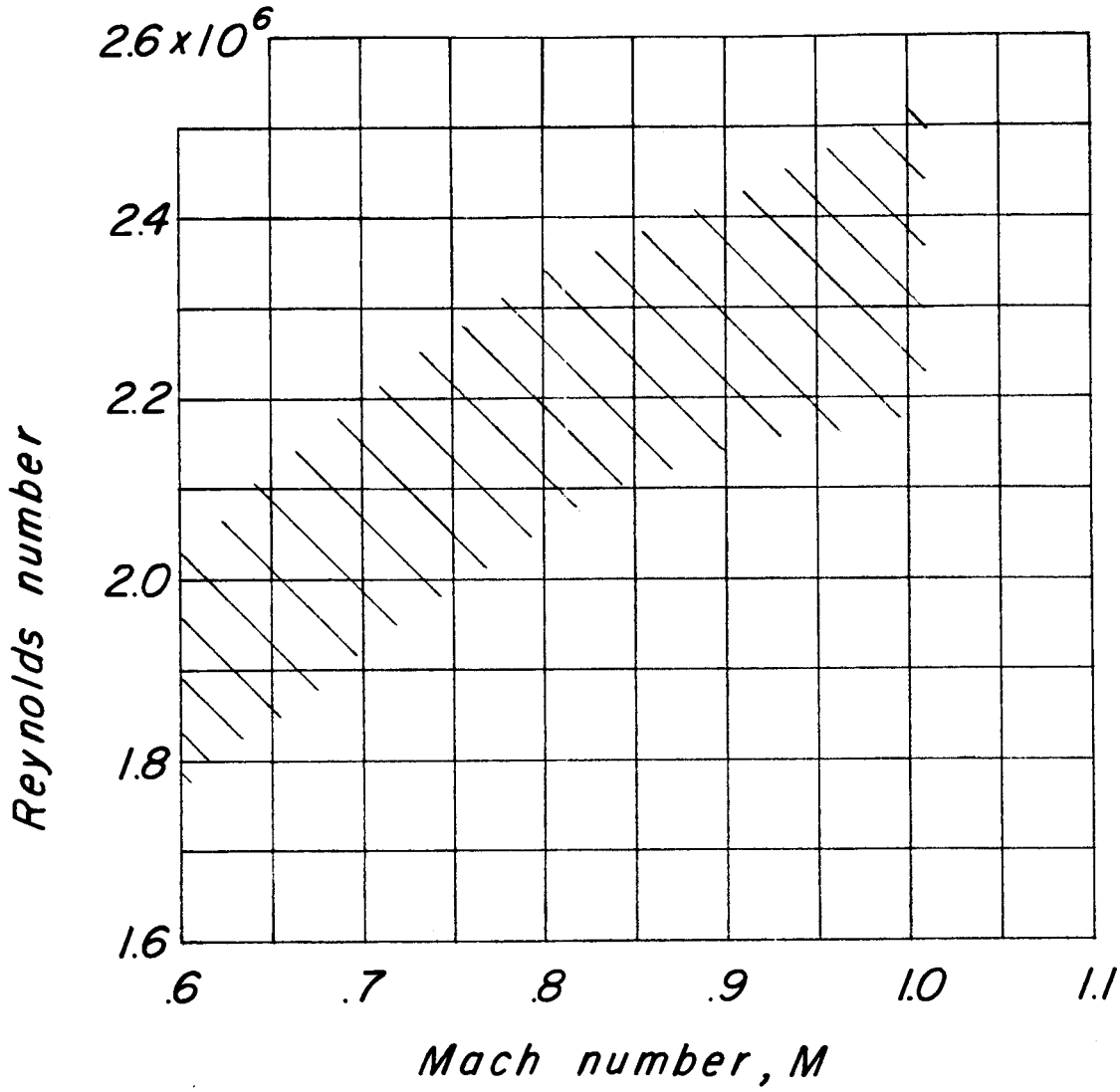

Figure 5.- Variation of Reynolds number with Mach number.

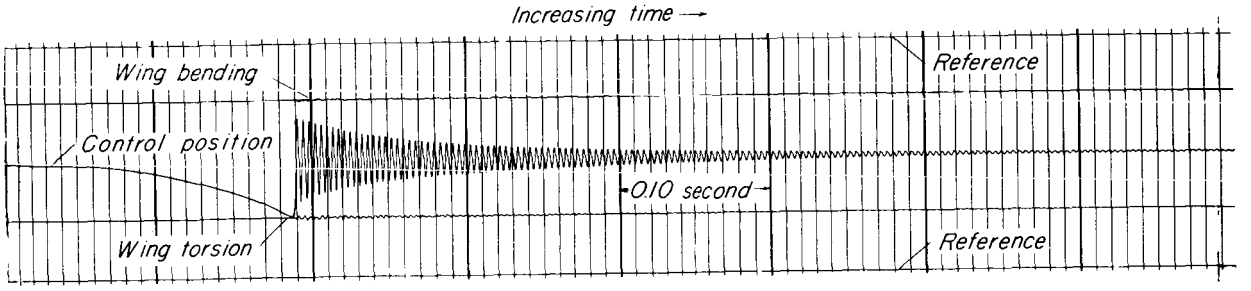

(a) Wind-off; control released at $\delta \approx 10^{\circ}$.

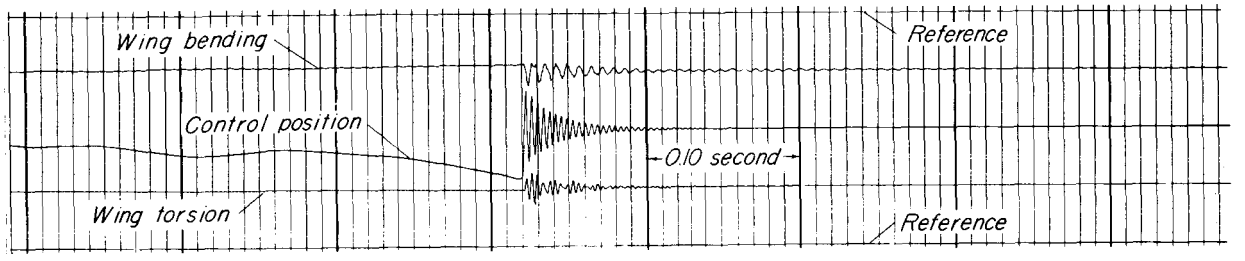

(b) M = 0.70; control released at $\delta \approx 10^{\circ}$.

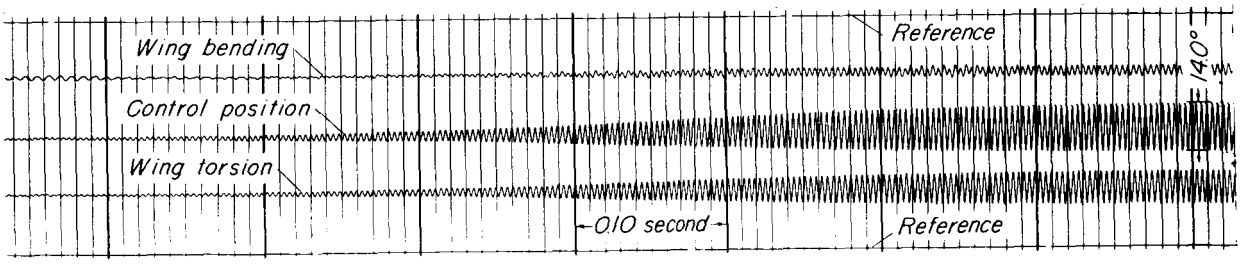

(c) M = 1.01; control released at $\delta \approx 0^{\circ}$.

Figure 6.- Typical oscillograph records. Light tip store; f_o = 260 cps; aspect-ratio-1.74 control.

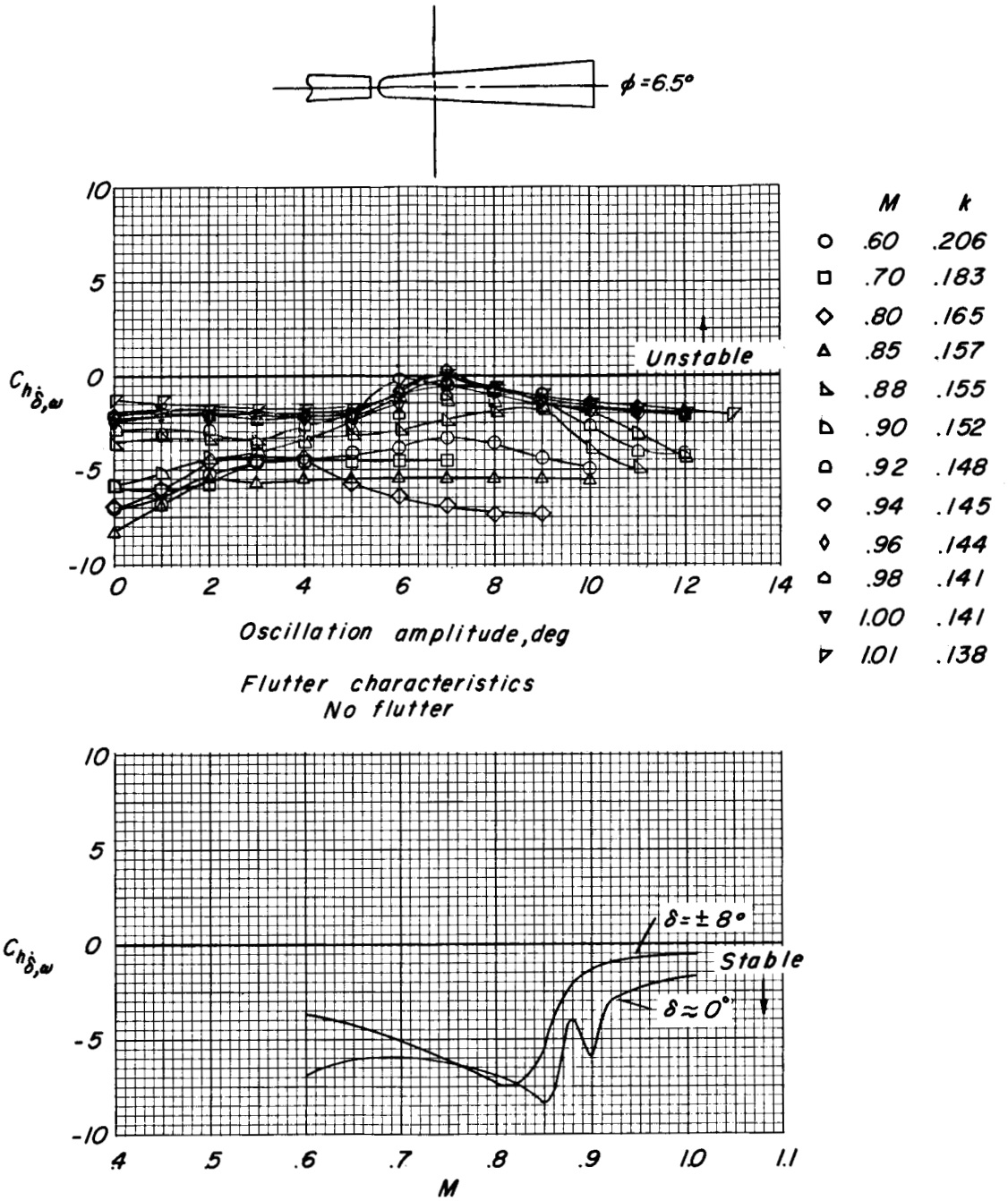

(a) f_o = 253 cps.

Figure 7.- Variation of damping derivative with oscillation amplitude and Mach number for various control frequencies. $\phi = 6.5°$ wedge control.

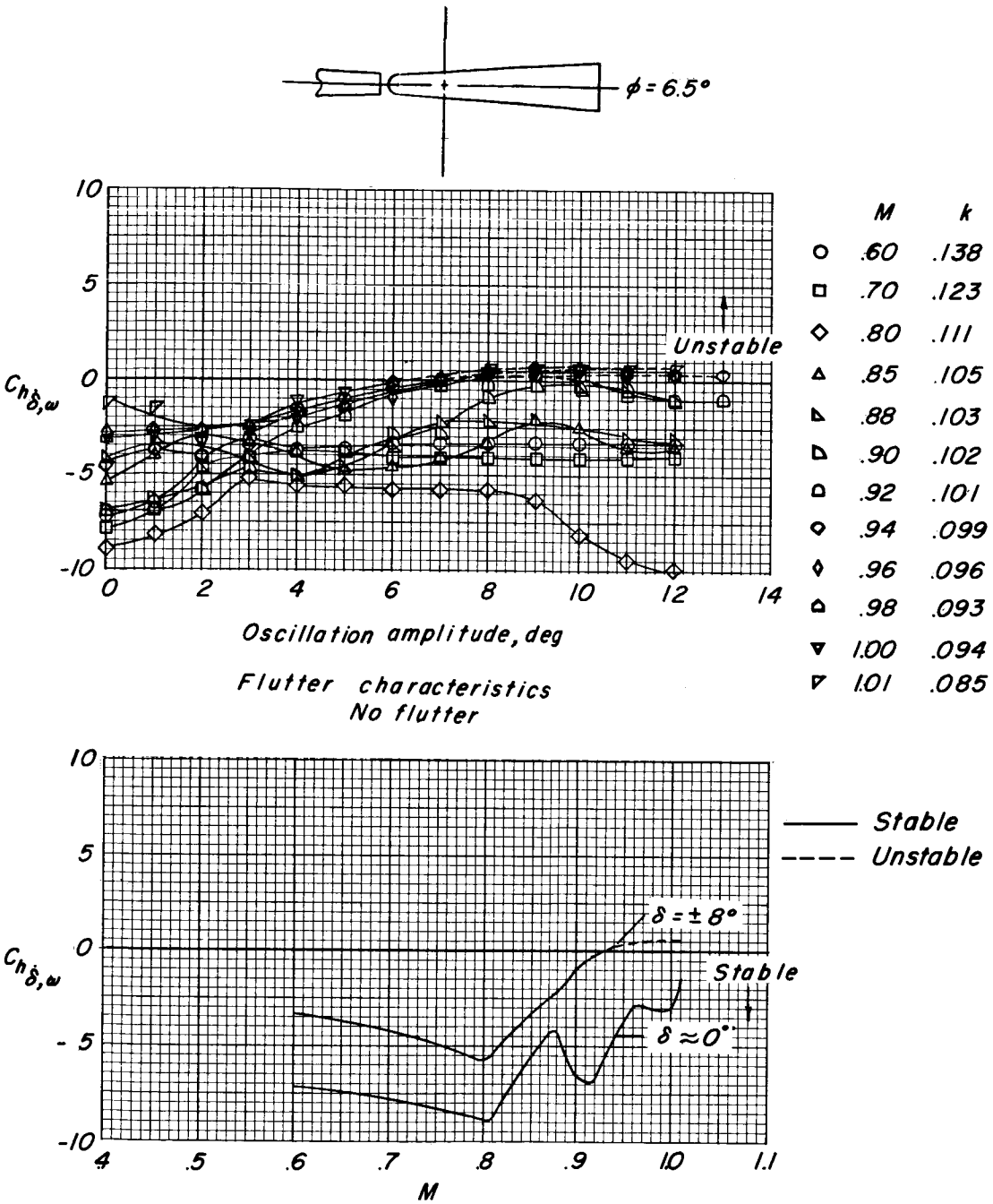

(b) f_o = 171.5 cps.

Figure 7.- Continued.

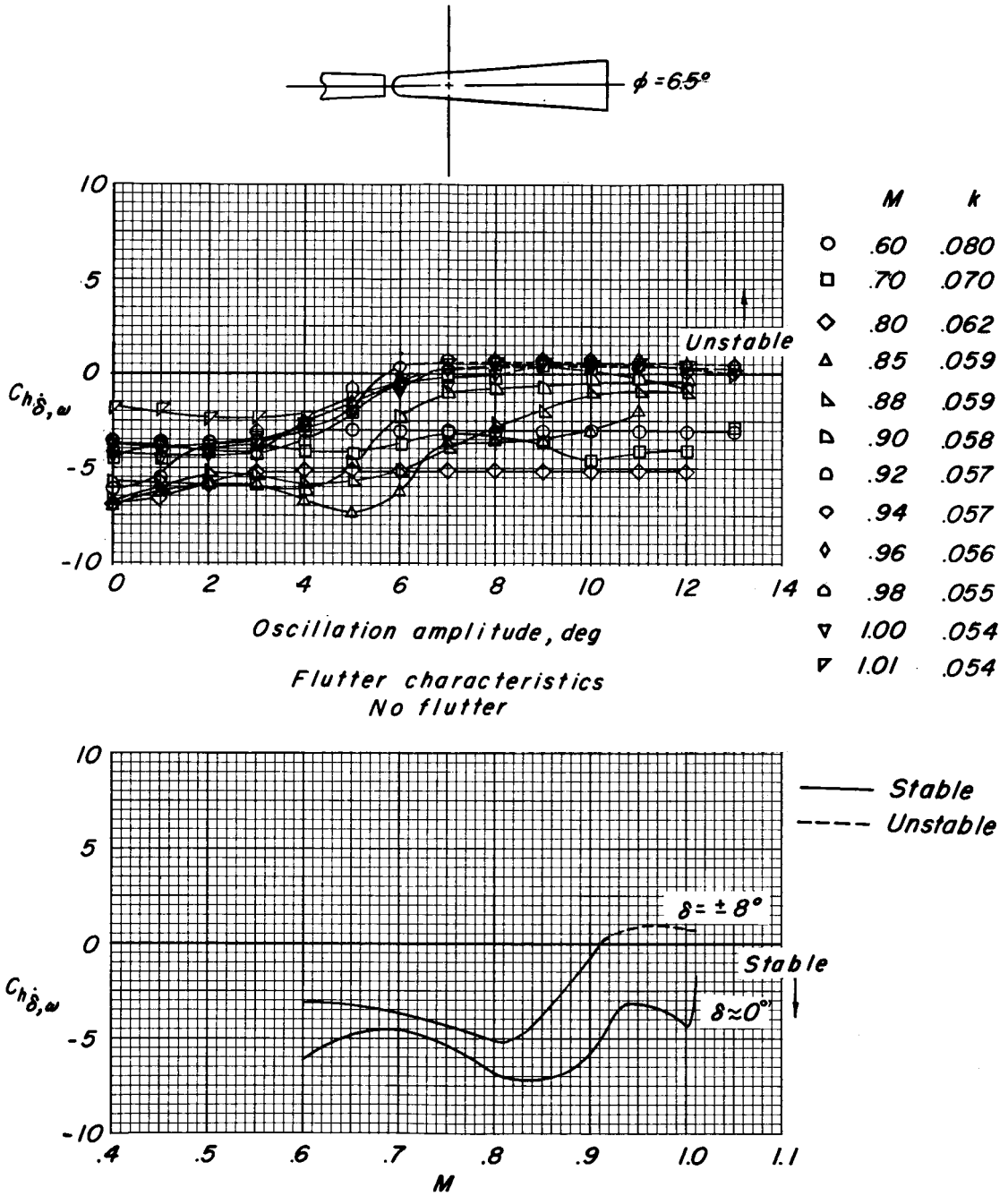

(c) f_o = 99 cps.

Figure 7.- Concluded.

[redacted]

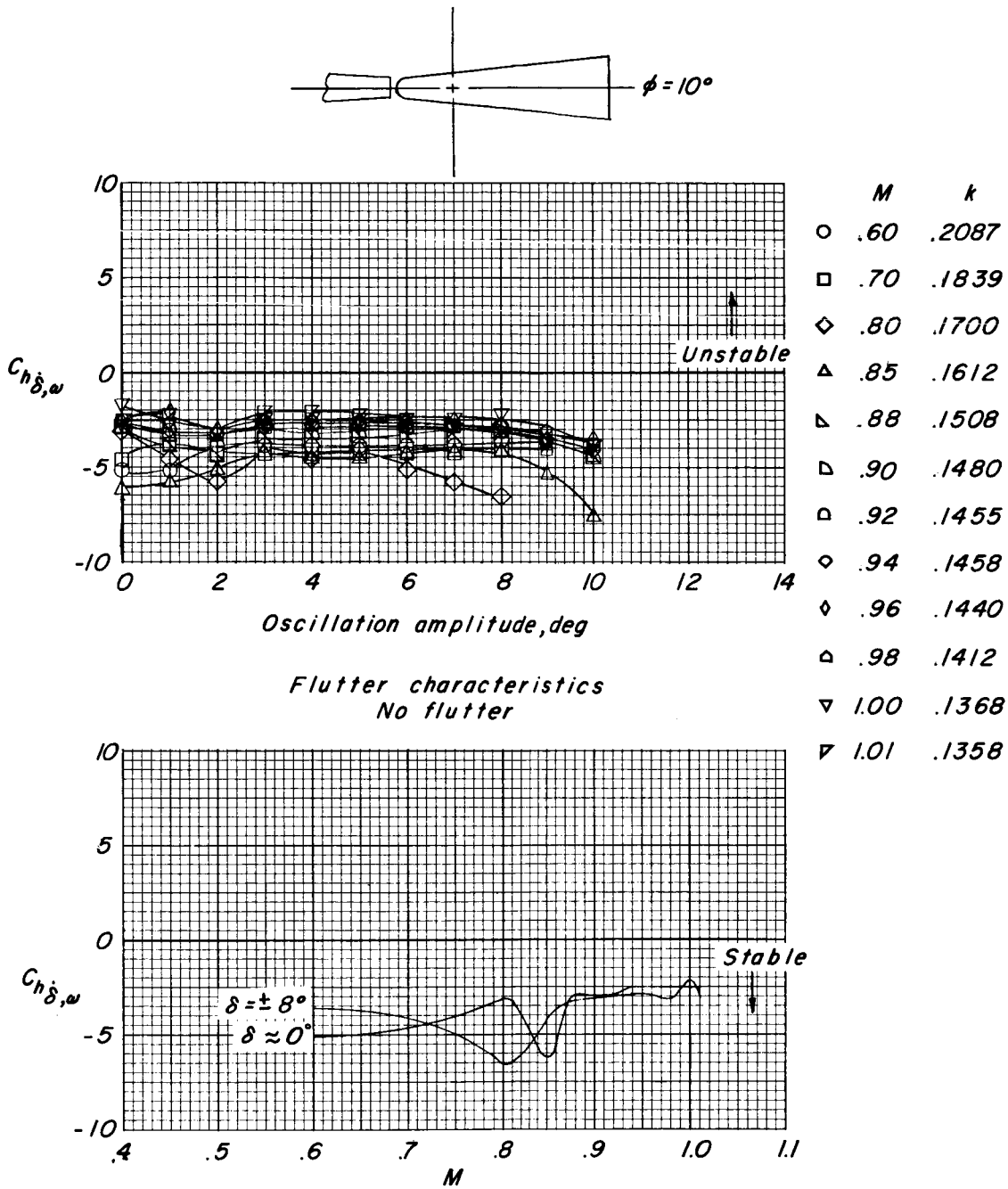

(a) f_o = 250 cps.

Figure 8.- Variation of damping derivative with oscillation amplitude and Mach number for various control frequencies. $\phi = 10°$ wedge control.

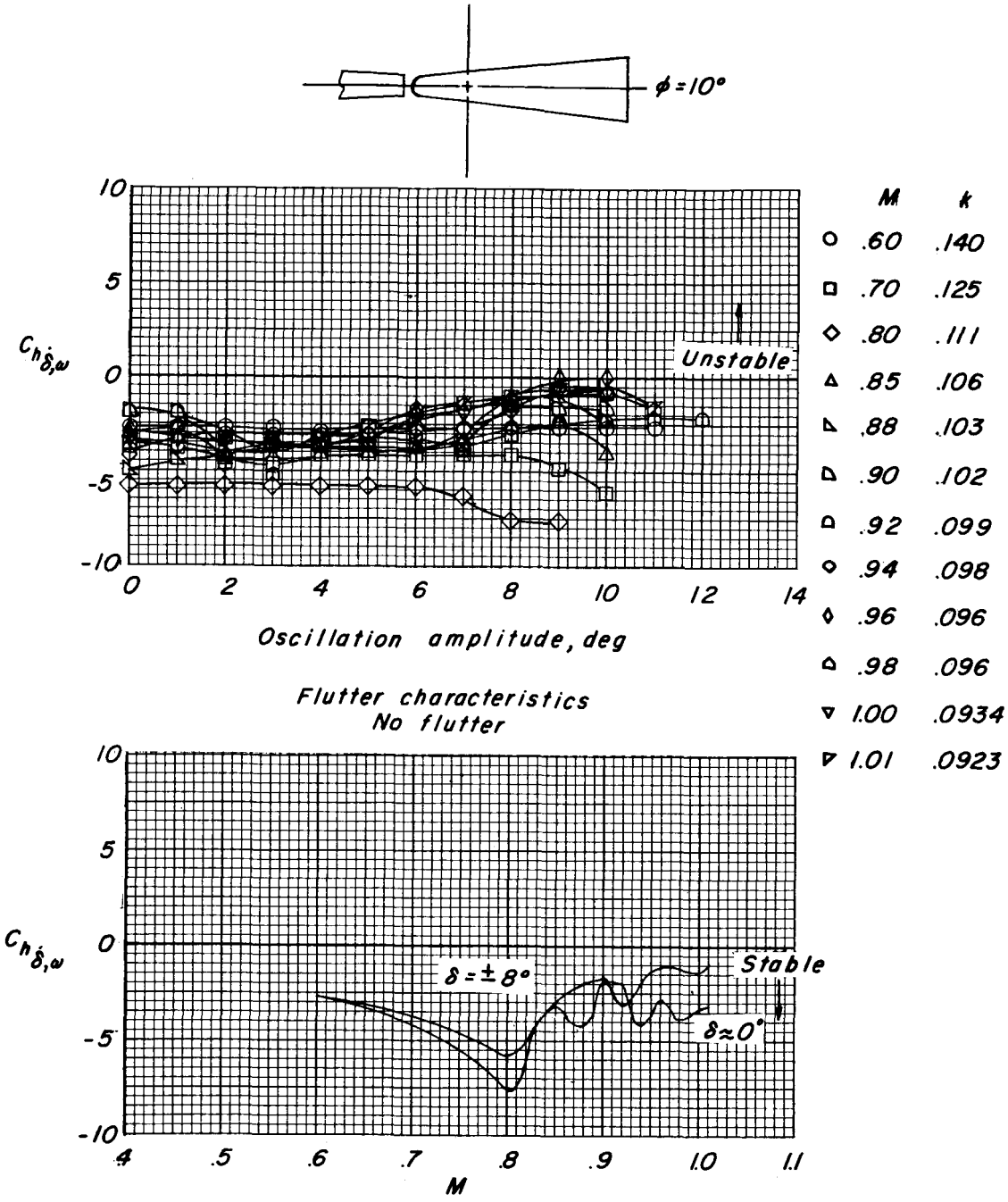

(b) f_o = 172.5 cps.

Figure 8.- Continued.

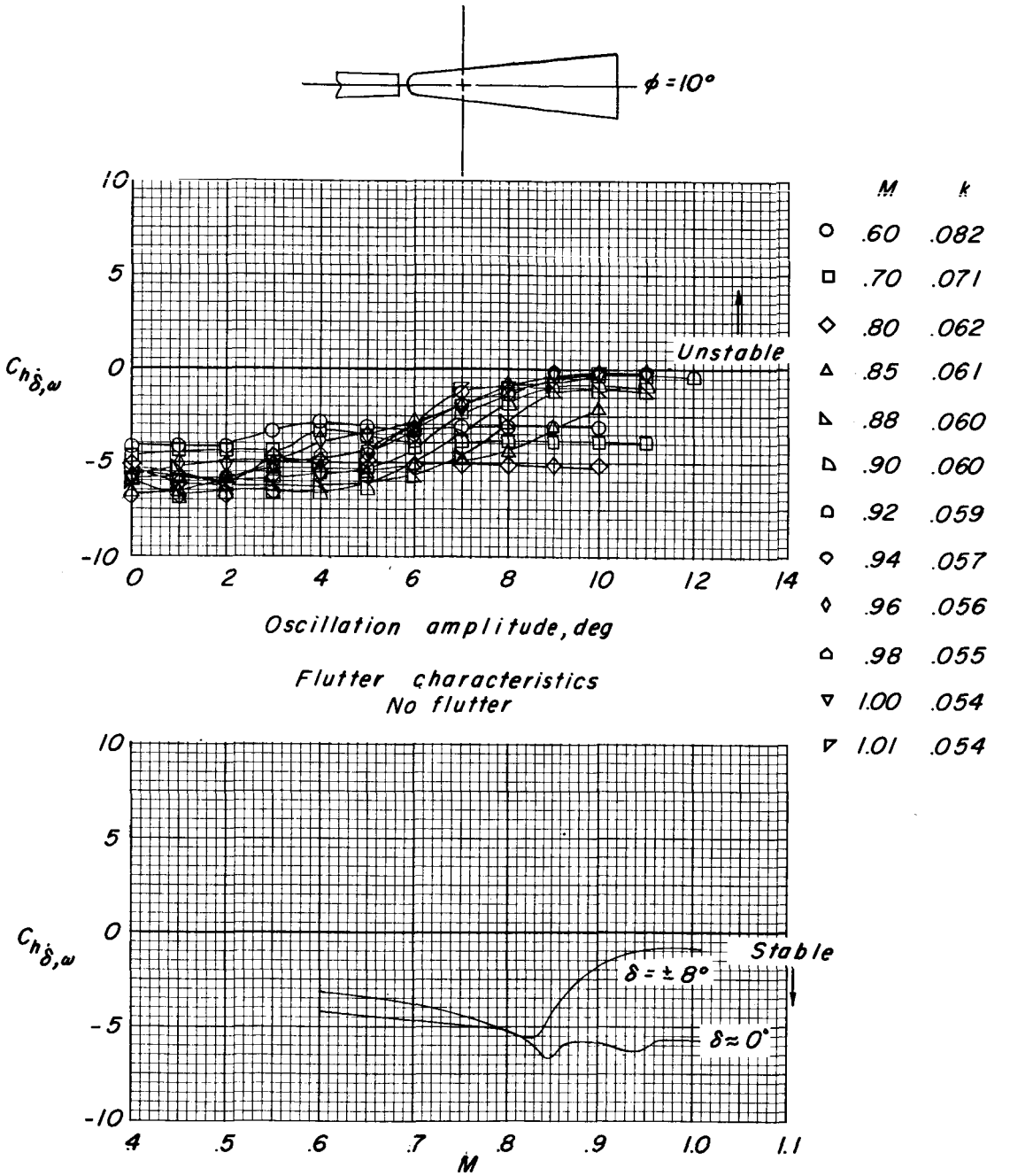

(c) f_o = 99 cps.

Figure 8.- Concluded.

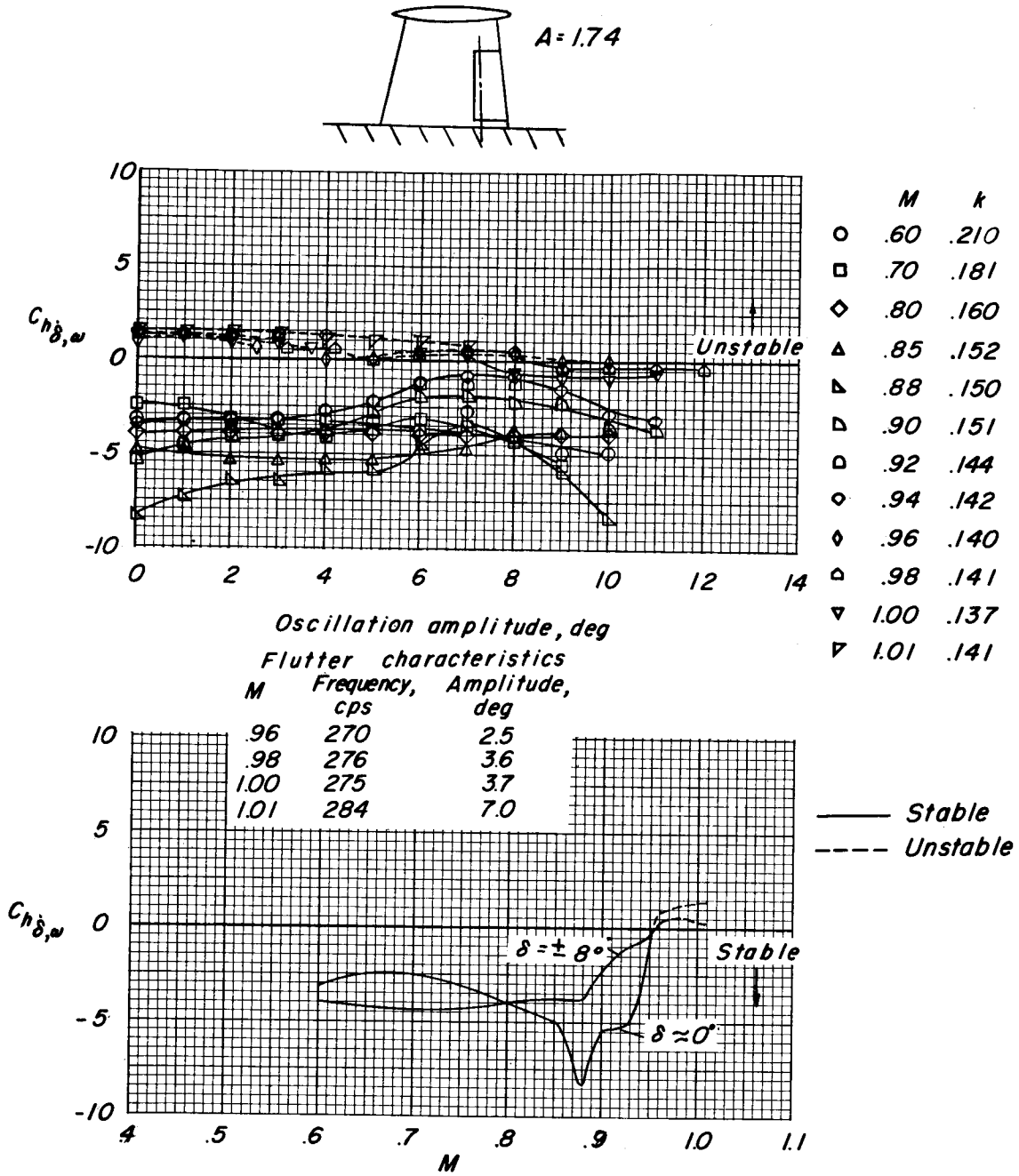

(a) f_o = 260 cps.

Figure 9.- Variation of damping derivative with oscillation amplitude and Mach number for various control frequencies. Aspect-ratio-1.74 control.

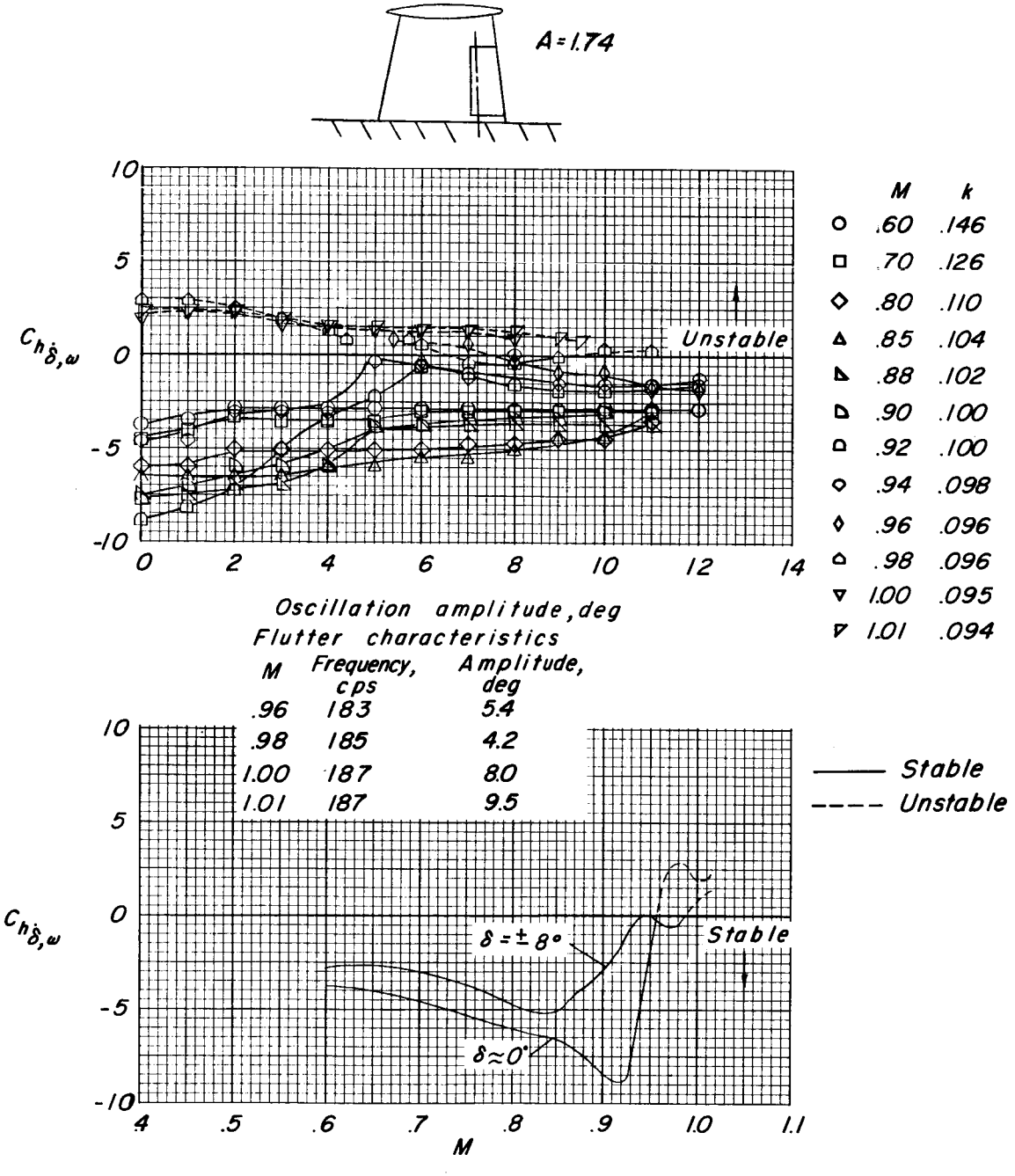

(b) f_o = 174 cps.

Figure 9.- Continued.

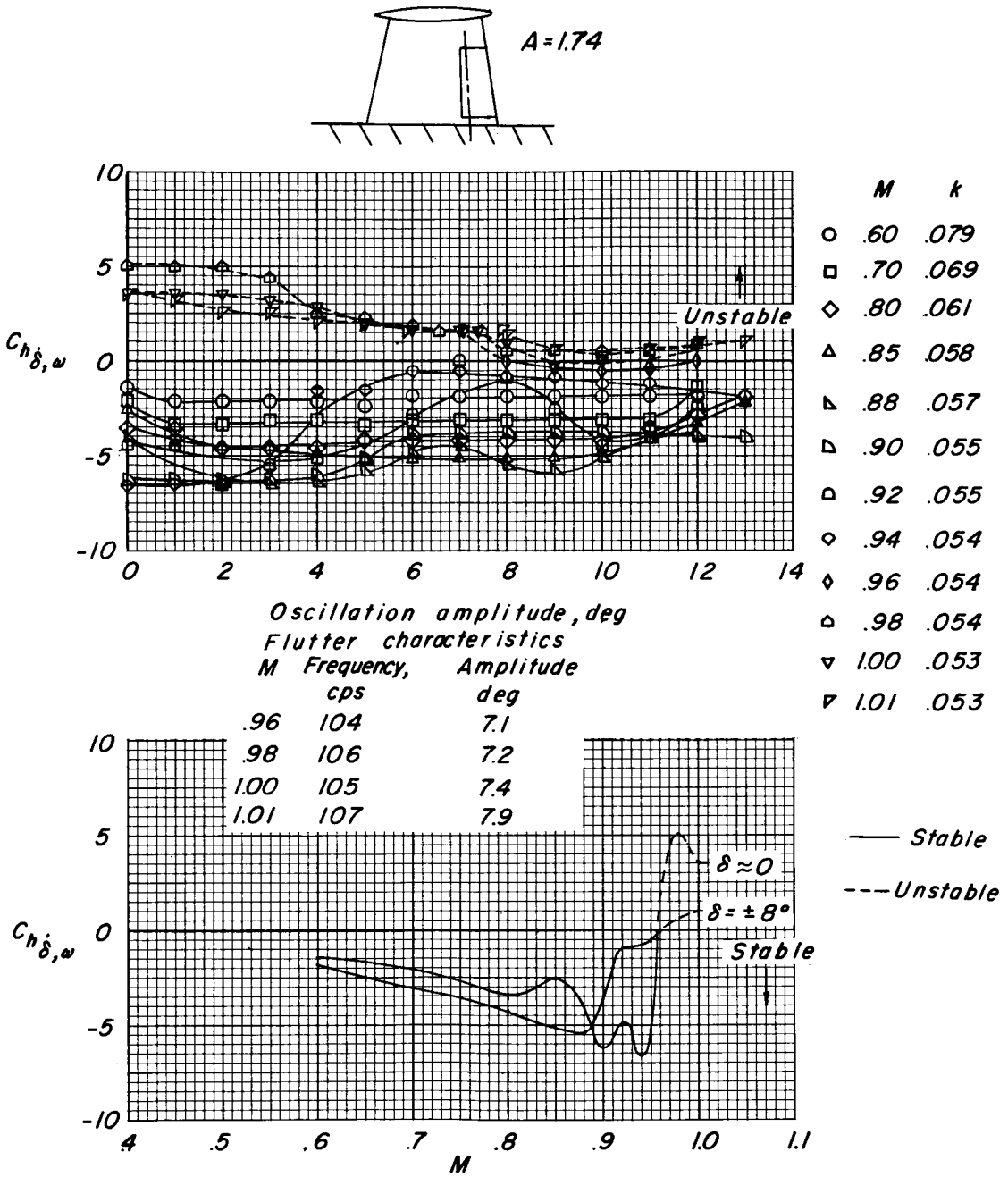

(c) f_o = 99.5 cps.

Figure 9.- Concluded.

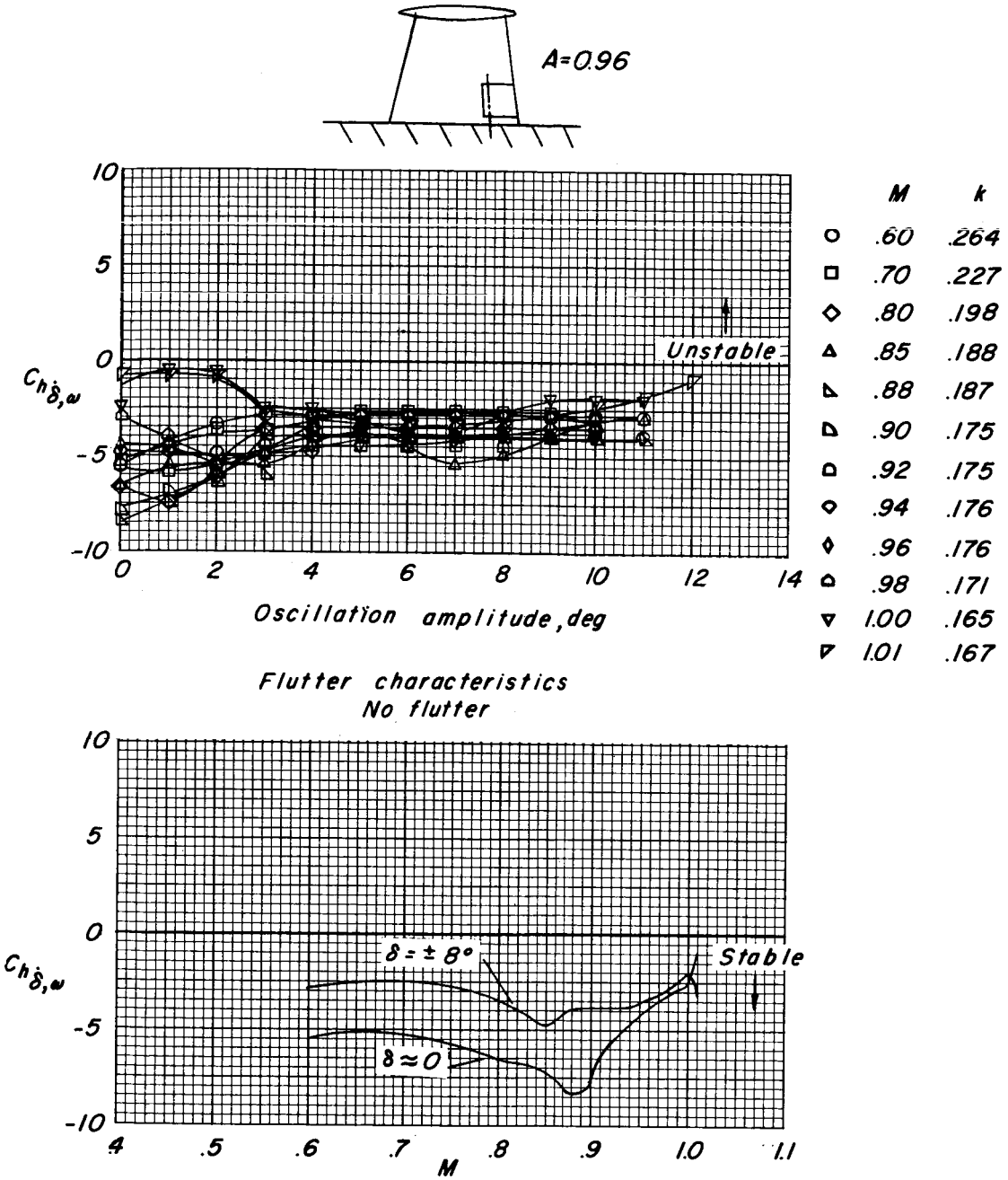

(a) f_o = 308 cps.

Figure 10.- Variation of damping derivative with oscillation amplitude and Mach number for various control frequencies. Aspect-ratio-0.96 control.

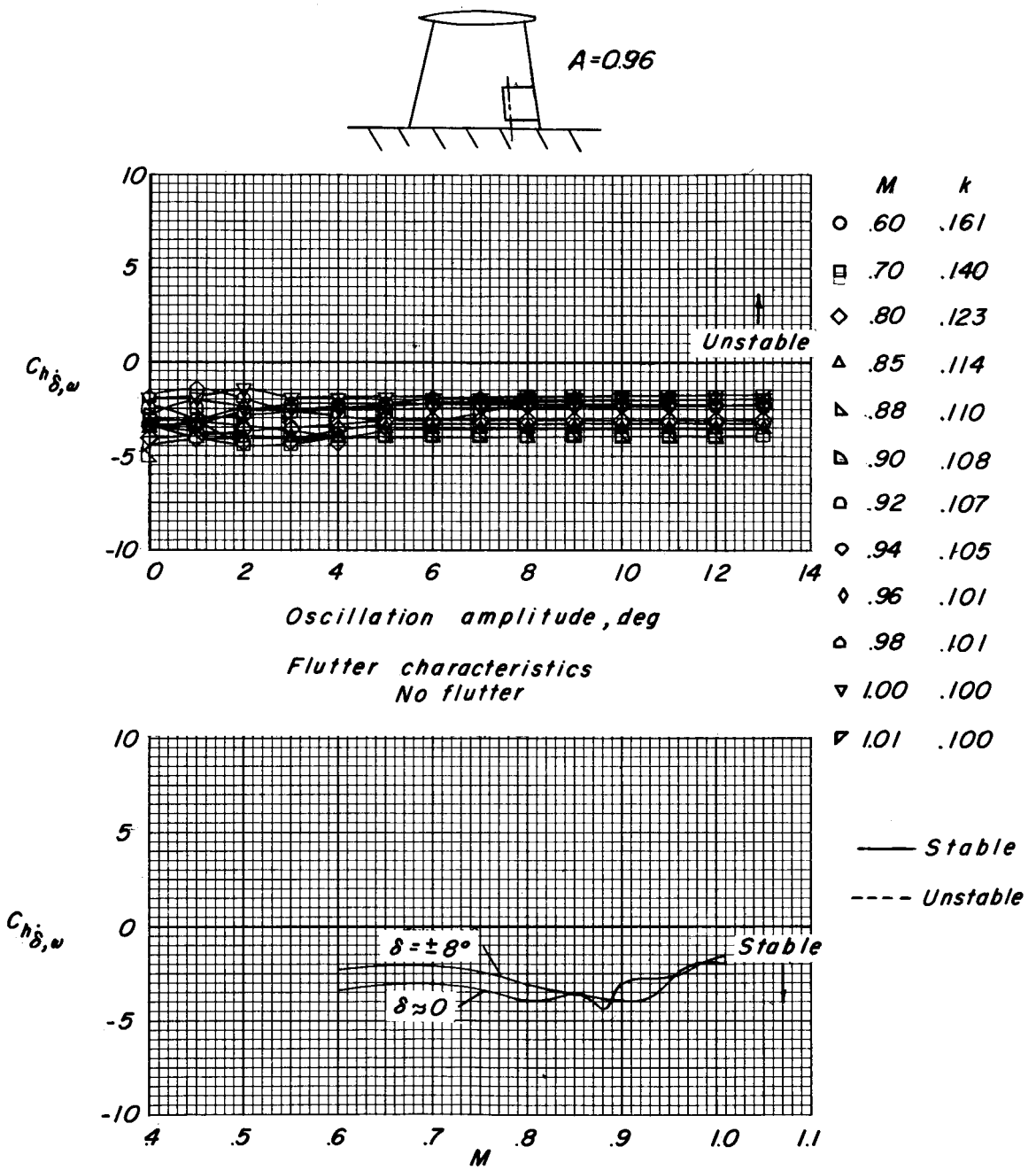

(b) f_o = 188 cps.

Figure 10.- Continued.

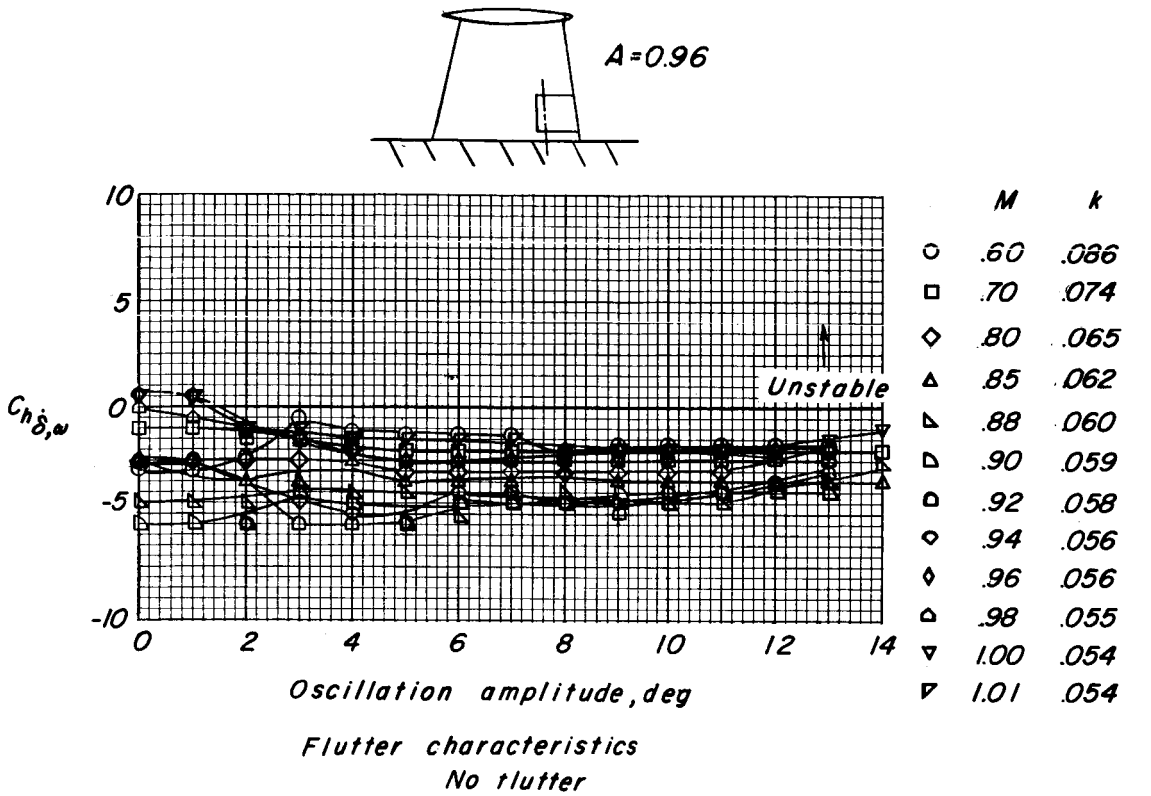

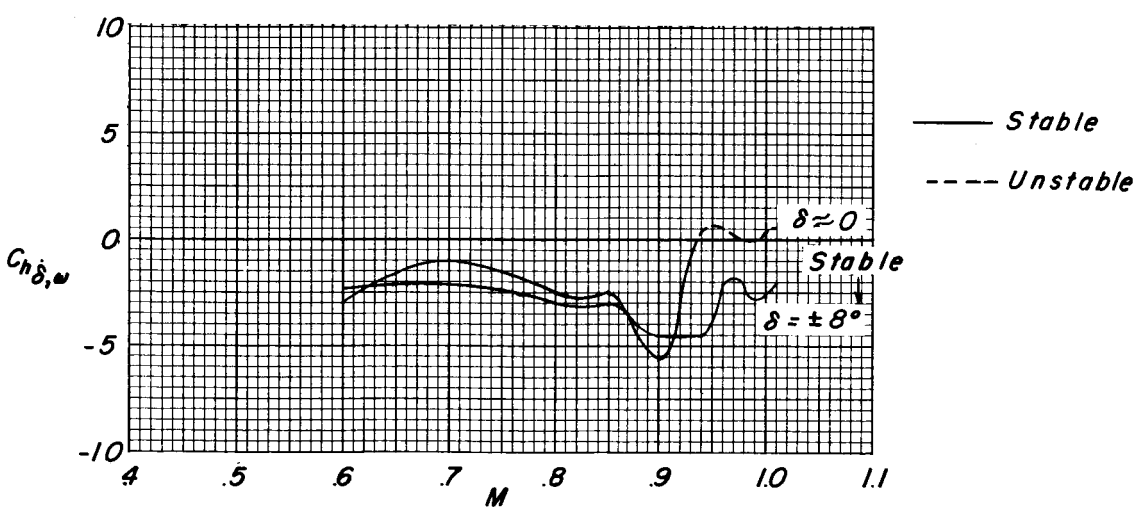

(c) f_o = 102 cps.

Figure 10.- Concluded.

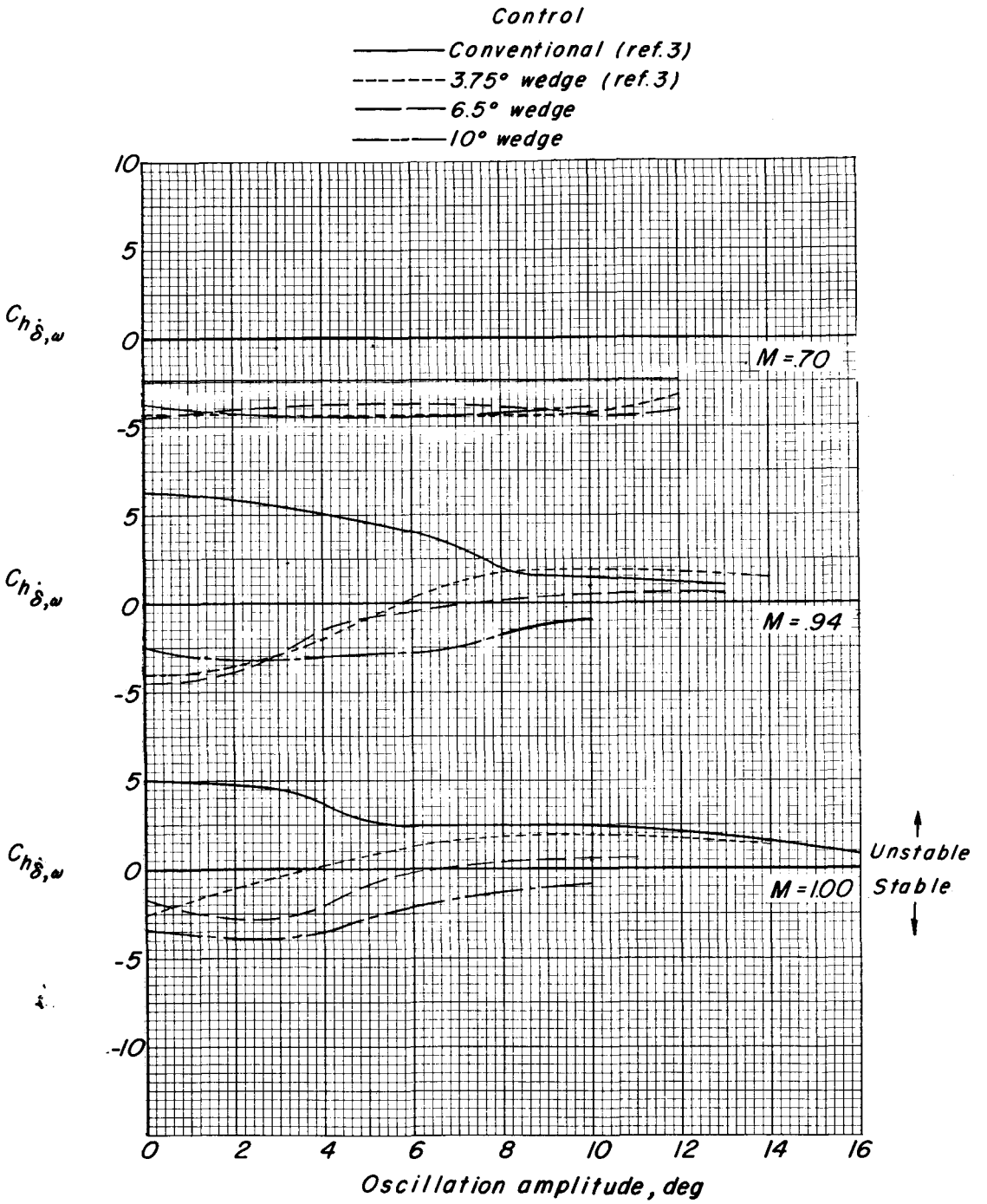

Figure 11.- Variation of damping derivative with oscillation amplitude for three representative Mach numbers and various wedge angles. $k \approx 0.10$.

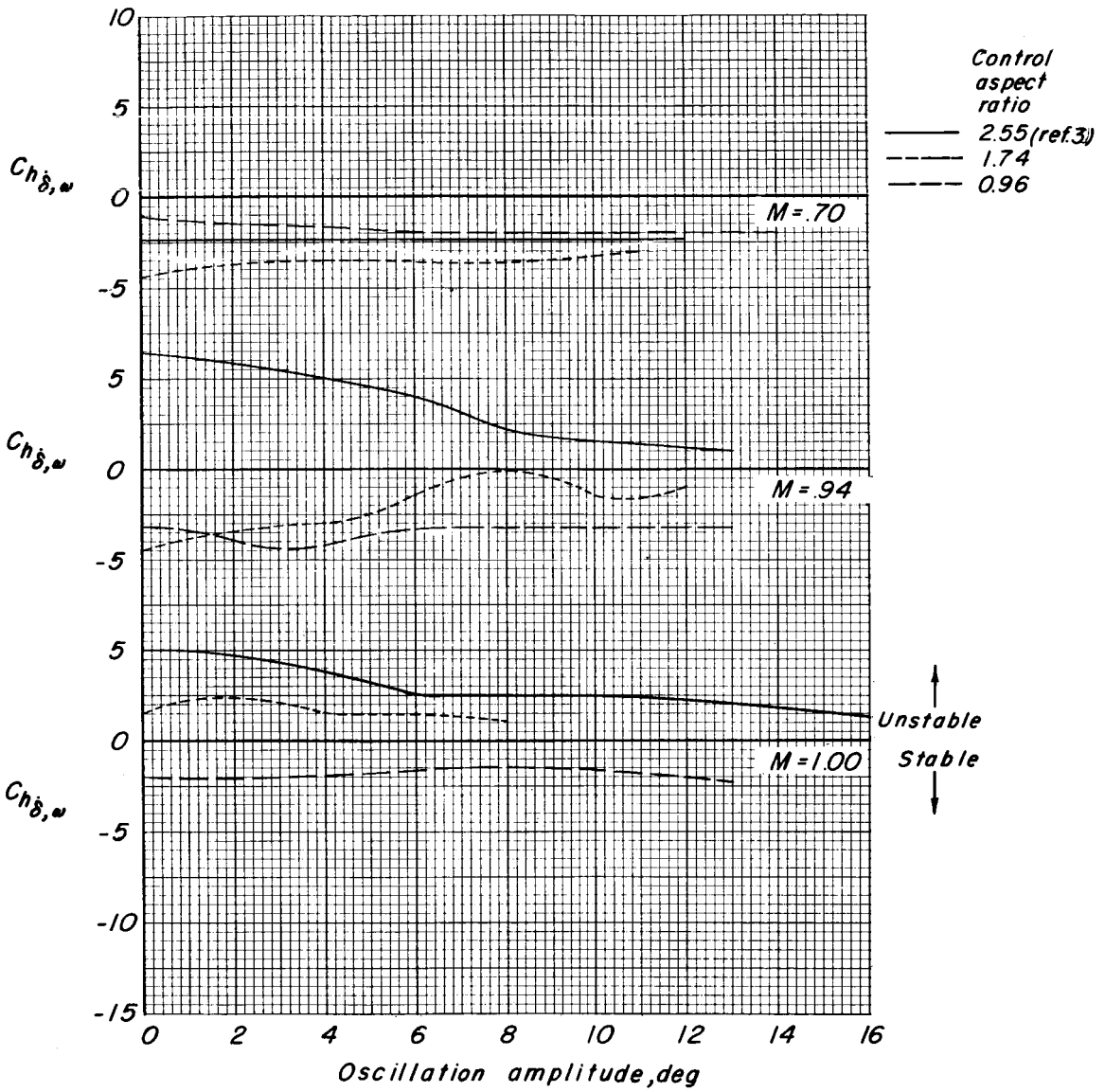

Figure 12.- Variation of damping derivative with oscillation amplitude for three representative Mach numbers and controls of various aspect ratio. $k \approx 0.10$.

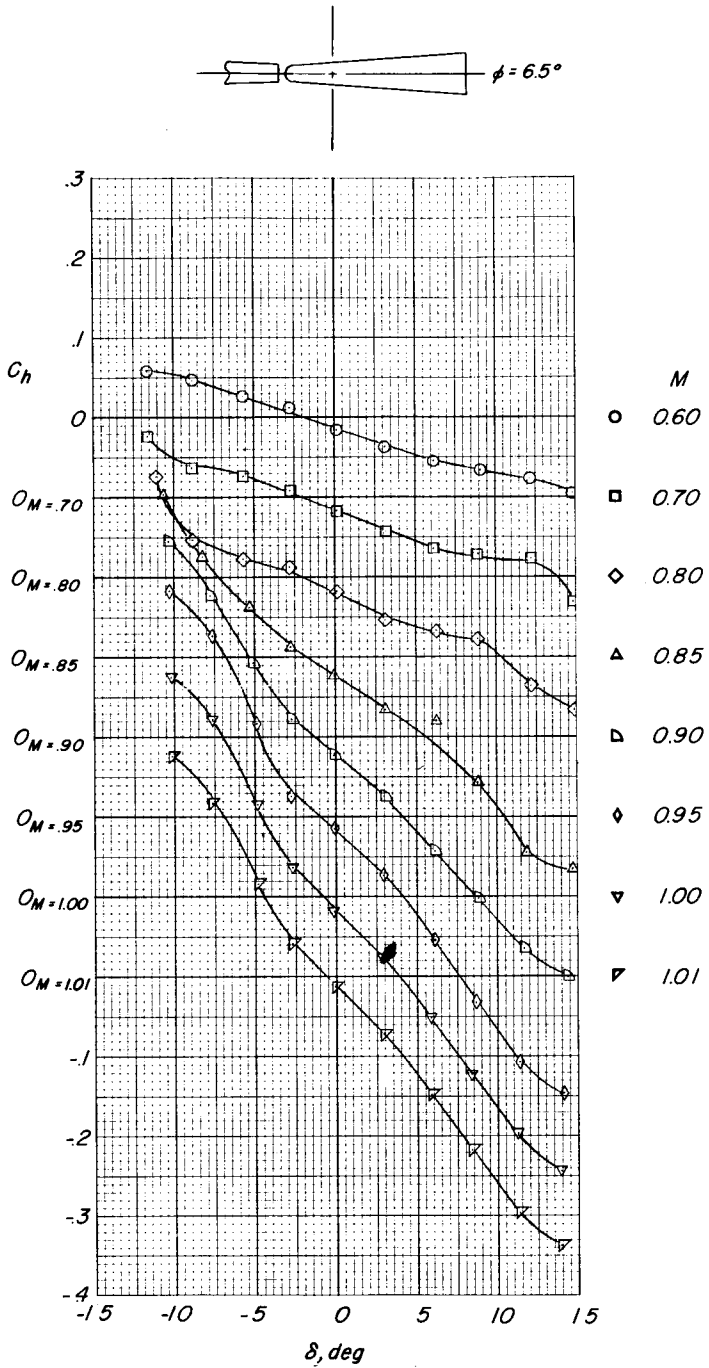

(a) $\phi = 6.5^{\circ}$ wedge control.

Figure 13.- Variation of static hinge-moment coefficient of wedge controls with control deflection for various Mach numbers.

[redacted]

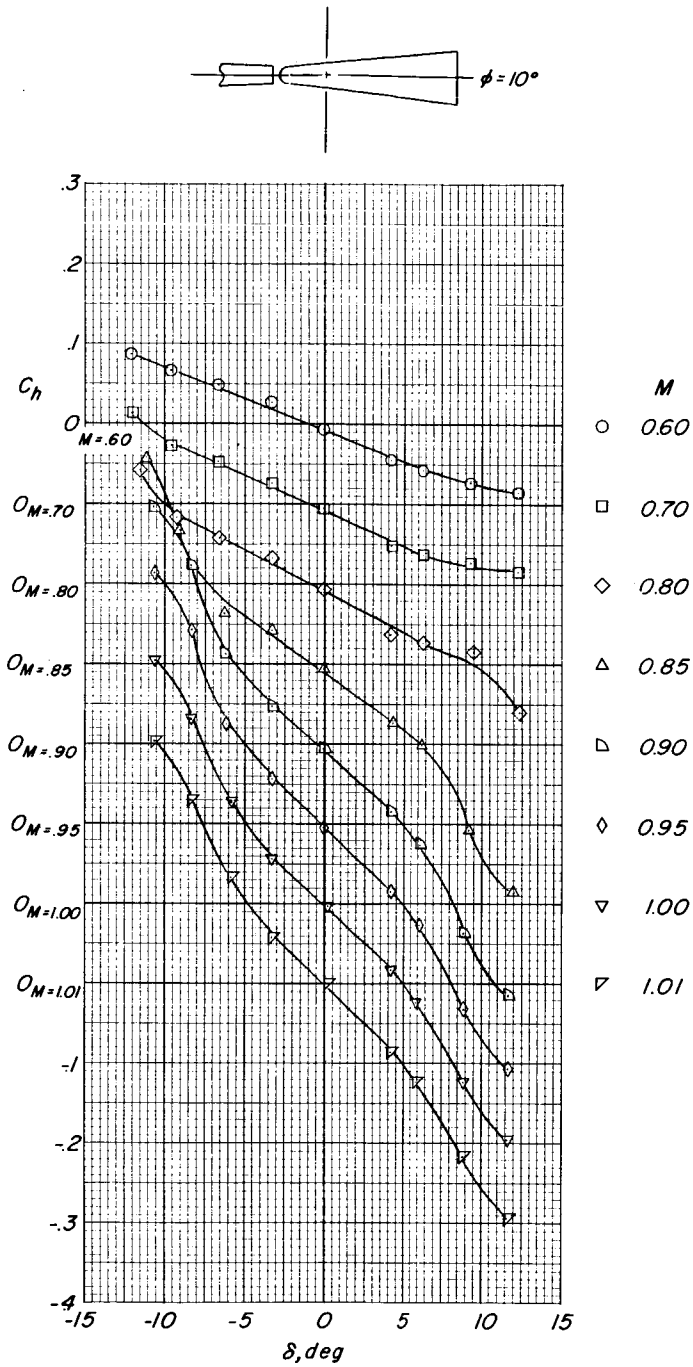

(b) $\phi = 10^{\circ}$ wedge control.

Figure 13.- Concluded.

[redacted]

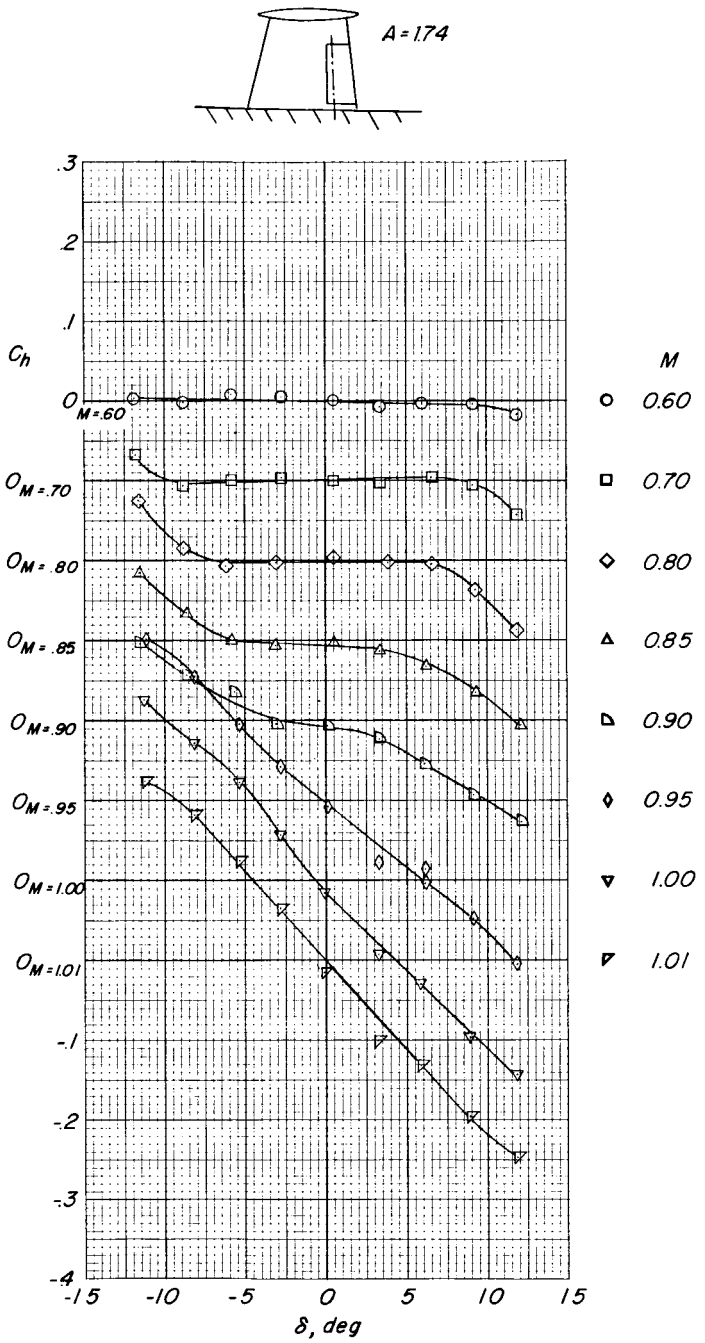

(a) Aspect-ratio-1.74 control.

Figure 14.- Variation of static hinge-moment coefficient of various-aspect-ratio controls with control deflection for various Mach numbers.

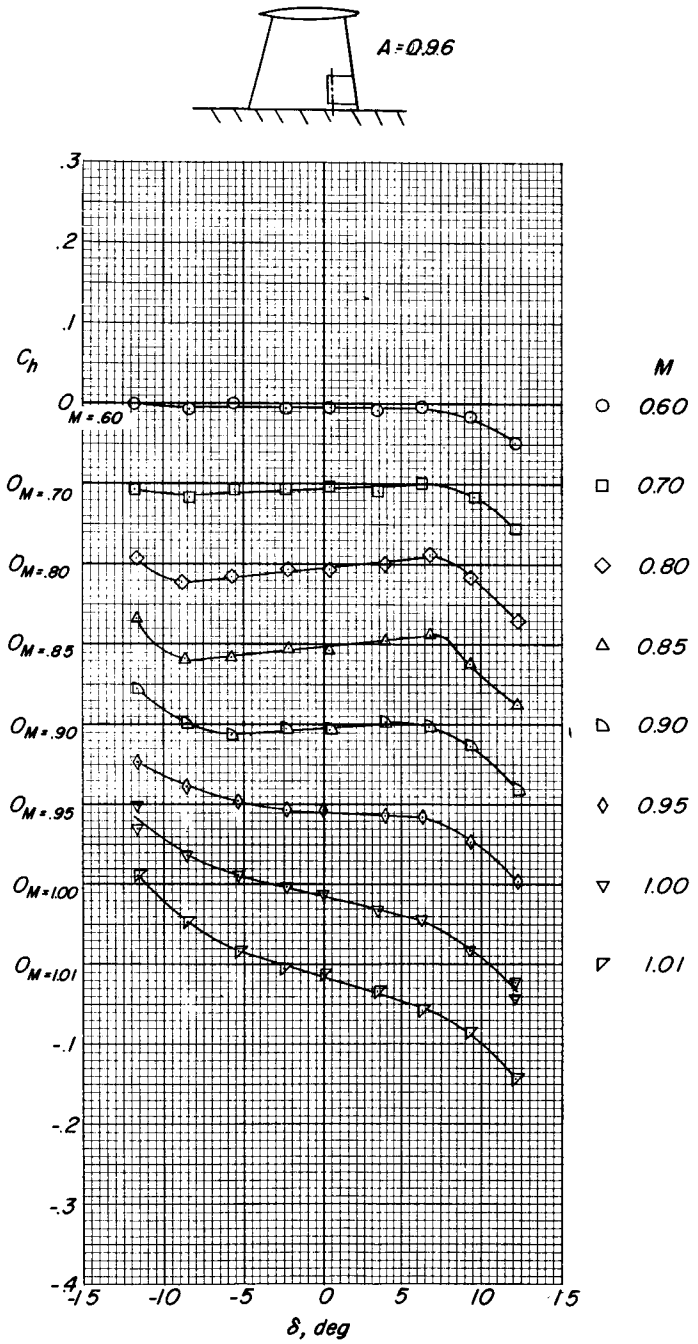

(b) Aspect-ratio-0.96 control.

Figure 14.- Concluded.

[redacted]

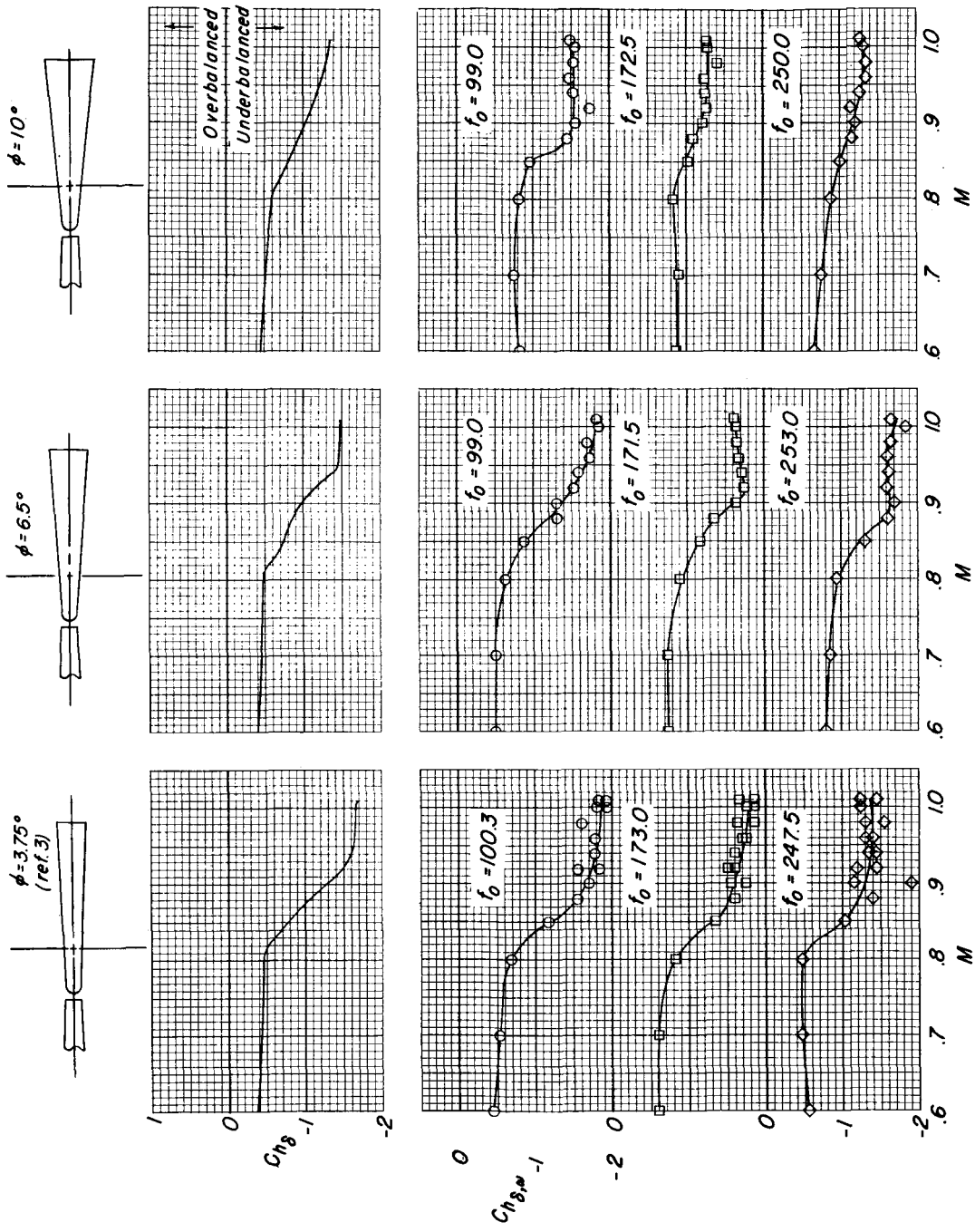

Figure 15.- Variation of C_{h_δ} and $C_{h_{\delta,\omega}}$ for controls of various wedge angles.

[redacted]

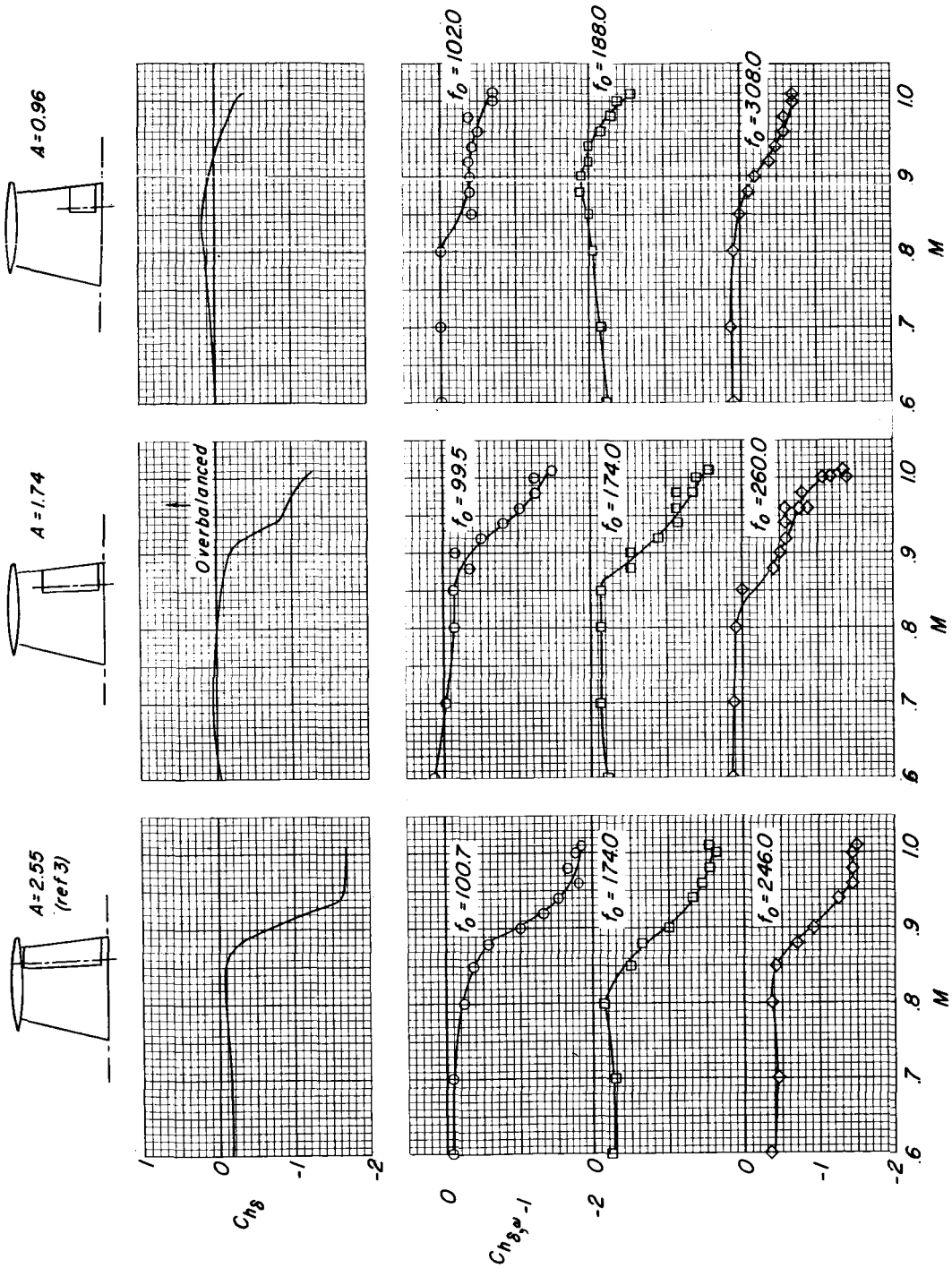

Figure 16.- Variation of C_{h_δ} and $C_{h_{\delta,\omega}}$ for conventional controls of various aspect ratios.

[redacted]